Modeling of the Coldfinger Water Exhauster for Advanced TEG Regeneration in Natural Gas Dehydration

Aalborg University Esbjerg
Oil and Gas Technology

Master´s Thesis

Iveth Romero
K10-OG-1-F19

Supervisors:
Marco Maschietti
Rudi P. Nielsen
Anders Andreasen

June 7, 2019

Contents

Abstract

The performance of natural gas dehydration using triethylene glycol (TEG) strongly depends on the purity levels of TEG in the regeneration unit. Coldfinger is a TEG regeneration technology reported to be capable of increasing TEG purity to levels above 99.8 wt.%, but conceptual models of this equipment appear to be lacking.

This work presents a methodology for modeling Coldfinger, where the equipment is represented as two theoretical equilibrium stages operating at different temperatures in the presence of internal vapor recirculation. The key parameters governing the functioning of the equipment are discussed on the basis of a series of simulations carried out for different top temperatures, internal recirculation ratios and stripping gas injection. The effect of the cooling efect of the Coldfinger is also analyzed through the quantification of the heat power exchanged by the system and its impact on the TEG purity levels achieved.

The conceptualization of the equipment functioning is first analyzed considering a simplified three-component system. Further analyses are performed by implementing the proposed Coldfinger modeling in the TEG regeneration stage of a gas dehydration unit where a multicomponent system is considered. The basis of comparison for quantification of the process efficiency is the behavior of a single-stage stripping process.

The results demonstrate that a regeneration of TEG up to approximately 99.9 wt.% is achievable by injecting smalls amounts of dry gas, considerably lower than conventional enhanced TEG regeneration by gas stripping.

Part of the work developed in this study was presented at the *14th International Congress on Chemical and Process Engineering* held in Bologna, Italy, on May 26th to May 29th 2019 organized by the *Italian Association of Chemical Engineering, AIDIC*, and published in the journal *Chemical Engineering Transactions*.

1 Introduction

Natural gas produced from reservoirs is often saturated with water. Additionally, downstream gas treatment processes like sweetening (removal of gaseous H_2S) use aqueous solutions that further saturate the gas with water. The presence of water above recommended levels can lead to serious operating and safety problems like the formation of solid hydrates, which can clog pipelines; the condensation of water during processing and transport causing slug flow and erosion; and potential corrosion of process facilities in the presence of sour gases like CO_2 and/or H_2S. For these reasons, dehydration of natural gas is important to achieve the required levels of water in the export gas stream and avoid the consequences before mentioned [1, 2].

Gas dehydration is the process by which water is removed from a gas stream to lower the dew point temperature of water. In common industrial practice, and when inhibition of hydrate formation is not possible [1], natural gas is dehydrated by absorption using liquid desiccants like triethylene glycol (TEG). Glycol solvents are the most popular liquid desiccants used for this purpose due to their strong affinity for water and relatively ease of regeneration.

The regeneration process consists of the transfer of water from the solvent (TEG) to the gas phase, thus recovering the solvent for reuse in the absorption process. In this way, the purity levels of TEG attainable in the regeneration stage have a strong effect on the efficiency of the absorption process. Regeneration is typically carried out by atmospheric distillation but it is limited to the glycol degradation temperature. In the case of TEG, regeneration at atmospheric pressure and 204.4 °C (close to TEG degradation temperature), leads to a TEG concentration of approximately 98.6 wt.% [1]. For this reason, several advanced regeneration processes have been implemented in oil and gas production to comply with current water content specifications, which means higher levels of TEG purity and consequently higher efficiency in the gas dehydration process [3].

One of these processes is the Coldfinger technology, which basically consists of a water exhauster integrated with the basic distillation column and fed by TEG leaving the reboiler. In the exhauster, TEG is further dehydrated by continuous vaporization coupled with partial condensation and removal of the vapor at the top of the equipment, where a cold pipe (i.e. the "cold finger") is located. It is typically reported that, using this technology, TEG purity around 99.2 to 99.5 wt.% is achievable [1].

Process modeling is a tool widely used for the design, analysis and/or optimization of processes as well as the conceptual design of unit operations through computer-based problem solving [4]. One of the principal objectives of process modeling is to understand the processes and equipment involved in the chemical industry, in order to evaluate and predict its behavior in an efficient way.

The Coldfinger water exhauster is an option for glycol regeneration that results attractive due to its theoretically simple installation and reduced consumption of stripping gas. However, to this day, available commercial process simulators are not provided with a Coldfinger unit *per se* and the modeling alternatives existent are somewhat limited or complex.

The dynamic behavior of the Coldfinger water exhauster increases the complexity of an accurate modeling of the unit. The continuous vaporization of the liquid along with the partial condensation of water and internal recirculation of the vapor produce a constant changing in its equilibrium state, reason why achieving an accurate steady-state modeling is challenging.

2 Problem Delimitation

The aim of this work is to develop a modeling alternative of the Coldfinger water exhauster based on phase equilibrium calculations. To achieve this objective, an in-depth study of the Coldfinger performance along with the influence of different parameters such as temperature of the cooling pipe, internal vapor recirculation rate and amount and composition of the injected dry gas are considered.

2.1 Problem Statement

Altogether, this work intends to lead to a better understanding and an accurate modeling of the Coldfinger technology.

A first estimation is performed through a self-defined routine in Matlab by considering the properties and conditions of the liquid (regenerated TEG) coming from the reboiler of the regeneration unit. Afterwards, the influence of the composition of the stripping gas on the TEG regeneration process is also analyzed. Finally, the concept of the modeling alternative is inserted in a simulation case in Aspen HYSYS® built under the same parameters and considerations of the self-defined routine, as part of a gas dehydration unit with triethylene glycol.

3 Theoretical Background

The common processes applied to dehydrate natural gas are absorption and adsorption. A less common method, but also used, is the nonregenerable dehydration with calcium chloride ($CaCl_2$) [5], which is mainly used for small gas flow rates in remote locations [2]. Dehydration by adsorption uses solid desiccants, like activated alumina, silica gel or zeolites, and is often used when very low dew points are required, for instance a cryogenic gas plant [6].

Dehydration by absorption is performed using liquid desiccants, i.e. solvents that have strong affinity for water. Among the numerous hygroscopic liquids available, few comply with the properties required in a good solvent for gas dehydration, which are [7, 8]:

- Highly hygroscopic
- Noncorrosive
- Easy regeneration
- Nonsoluble/low solubility in liquid hydrocarbons
- Thermal stability
- Low affinity for acid gases
- Low cost
- Low toxicity

Glycol solutions are the solvents that comply with the majority of such properties. Four glycols have demonstrated a good performance in natural gas dehydration: ethylene glycol (EG), diethylene glycol (DEG), triethylene glycol (TEG) and tetraethylene glycol (TREG). Table 3.1 summarizes their principal physical properties [8].

Table 3.1: Physical properties of different glycol solutions

Property	EG	DEG	TEG	TREG
Boiling point at 101325 Pa (°C)	197.30	245.00	277.85	307.85
Vapor pressure at 25 °C (Pa)	12.24	0.27	0.05	0.007
Absolute viscosity @ 25 °C (Pa s)	0.018	0.030	0.037	0.043
Absolute viscosity @ 60 °C (Pa s)	0.005	0.008	0.009	0.010
Flash point (°C)	111.1	123.89	176.67	196.11

Of the four glycols available, triethylene glycol (TEG) has been widespread used in the industry. As it can be seen in Table 3.1, the boiling point temperature of TEG at atmospheric pressure is higher than that of EG and DEG; thus, it can be easily regenerated to concentrations up to 99 % with atmospheric distillation [2]. Additionally, TEG has lower vaporization losses, higher dew-point depressions of natural gas [2], and higher initial theoretical decomposition temperature of approximately 206 °C [7]. Even though TREG presents the most optimal properties of the four glycols, it is more expensive; therefore, TEG is commonly selected for gas dehydration processes [2].

TEG has been commonly used to dehydrate sweet and sour gases over a wide range of operating conditions. For instance, at an operating pressure range of 0.3 MPa to 17 MPa and a temperature range of 4 °C to 71 °C, the gas dew point depression achievable with TEG ranges between 4 °C to 60 °C [9].

3.1 Dehydration Process Description

Figure 3.1 shows a basic glycol dehydration unit, extensive to any type of glycol used. The system is divided into the two main processes involved: gas dehydration (absorption process) and glycol regeneration.

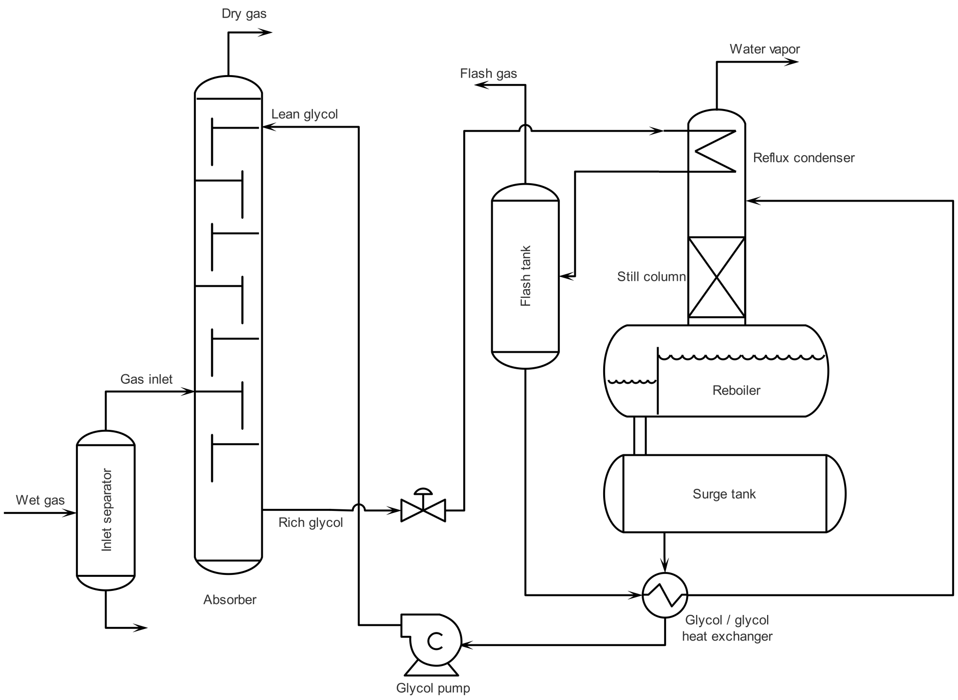

Figure 3.1: Process flow diagram of a gas dehydration process with glycol.

Wet gas enters the dehydration process through the inlet separator, which removes the liquid water, hydrocarbons or treating chemicals of the wet gas stream before entering the absorption process. Good engineering practice recommends installing such separator upstream the absorber, even when an integral separator at the bottom of the absorber exists, for a satisfactory performance of the column [1]. The integral separator is not intended to replace the inlet separator and both devices act as complement of each other [2].

In the absorption process, water is removed from the gas stream by counter-current contact with the glycol in a trayed or packed column, named absorber or contactor, interchangeably. Thus, the wet gas enters the bottom of the absorber and the lean glycol (without water) enters at the top of the column, by the top tray or the top of the packing.

As glycol flows downwards the column, absorbs the water from the up-flowing wet gas stream. In this way, the dehydrated gas leaves the column at the top and the glycol, full with water, leaves at the bottom.

It is reported that a good gas dehydration can be achieved when the absorber operates at constant pressure, up to 20 MPa [5], and low temperatures, up to 38 °C to avoid glycol losses [8]. On the other hand, the regeneration stage is usually carried out at atmospheric pressure and temperature below the decomposition temperature of the chosen glycol [8]. Due to this difference in operating conditions, upon leaving the dehydration column, the rich glycol must increase its temperature and reduce its pressure before entering the regenerator. This is accomplished with a pressure-reduction valve generally located on the exit stream at the bottom of the absorber, and the gradual heating of the rich glycol by heat exchange with the hot streams of the process.

The rich glycol (glycol with water) leaving the bottom of the column enters the regeneration process through the reflux condenser located at the top of regeneration column, also called still column, regenerator or reconcentrator, to increase its temperature. Then, the rich glycol enters the flash drum, which consists of a three-phase separator that removes the dissolved gases of the liquid stream and any hydrocarbon. It is important to pre-heat the rich glycol before entering the flash drum to reduce its viscosity and make the gas/liquid separation easier [6]. Upon leaving the flash drum, the rich glycol enters the glycol filters, consisting of a sock filter and an activated carbon filter arranged in series. Here, the solid particles and the liquid-entrained hydrocarbons and/or dissolved contaminants are removed, respectively.

Before entering the regeneration column, the rich glycol flows through the glycol/glycol heat exchanger, where its temperature is further increased by indirect contact with the hot lean glycol (without water) leaving the regeneration process. The aim of this heat exchanger is to reduce the heat duty of the regeneration column.

Downstream the glycol/glycol heat exchanger there is the regenerator, consisting of the regeneration column and reboiler, where water is removed from the rich glycol by distillation thus, increasing the glycol concentration to the required value. The rich glycol enters the regeneration column at the top and flows down through the stripping section to the reboiler, increasing its temperature. The gas flashing from the liquid stream is mainly water with small amounts of glycol. The vapors leaving the regeneration column meet the reflux condenser at their exit, which decreases their temperature due to the cold rich glycol flowing through the condenser, leading to the condensation of the glycol carried with the water vapor. The condensed glycol goes back down to the reboiler, preventing in this way excessive vaporization losses. The reboiler containing the regenerated (lean) glycol supplies the necessary heat to the regeneration column to remove the water. For this purpose, the reboiler is provided with a fire tube for direct heating of the glycol. From the reboiler, the lean glycol flows to the surge tank, then to the glycol/glycol heat exchanger and finally it is pumped back to the absorber to start again the dehydration/regeneration cycle.

Since the rich glycol is directly heated in the reboiler, an important factor to take into consideration is its decomposition temperature, which will limit the reboiler set temperature. According to Campbell [7], the initial thermal decomposition temperatures of glycols are the ones shown in Table 3.2. The glycol leaving the reboiler is at its bubble point.

Table 3.2: Thermal decomposition temperature of different glycol solutions

Glycol	Temperature, °C
Ethylene glycol, EG	165
Diethylene glycol, DEG	164
Triethylene glycol, TEG	206
Tetraethylene glycol, TREG	238

3.1.1 Operating Parameters

The operating parameters of the basic glycol dehydration unit with TEG are summarized in Table 3.3.

Table 3.3: Operating parameters

Parameter	Value	Reference
Glycol circulation rate	27 L TEG/kg H_2O	[1]
Absorber temperature min/max	10/38 °C	[8]
Absorber pressure min/max	4/8 MPa	[6]
Absorber number of trays	6 to 8	[2, 5, 6]
Still column top temperature min/max	99/107 °C	[2, 5]
Reboiler temperature	193-204 °C	[1, 5]
Regenerator pressure	atmospheric	[7]
Flash drum pressure min/max	0.4/0.6 MPa	[1, 2]
Flash drum temperature min/max	38/66 °C	[2]
Glycol/glycol heat exchanger approach (hot end)	15-20 °C	[7]
Lean glycol to pump max temperature	60-65 °C	[7]
Lean glycol to absorber temperature approach	5.6-8.3 °C	[5]

The TEG dehydration unit operated under the above recommended parameters will most likely reach a regeneration of TEG up to 98.6 wt.% [1].

3.2 Enhanced Glycol Regeneration

Higher concentrations of TEG are typically achieved by the injection of stripping gas or the application of advanced glycol concentration processes like the Drizo® or the Coldfinger® process.

The Drizo process applies azeotropic distillation with iso-octane [2], which can be either recovered from the rich TEG upon the absorption process or supplied from an external source [1]. This process allows high stripping gas flow rates and subsequent high TEG concentrations.

3.2.1 Stripping gas injection

Stripping gas injection is the most common method used to increase TEG concentration in the regeneration process. It can be injected directly into the reboiler through a sparge line located at the bottom or it can be injected into a stripping column (also *Stahl column*) connected between the reboiler and the surge tank [1, 7].

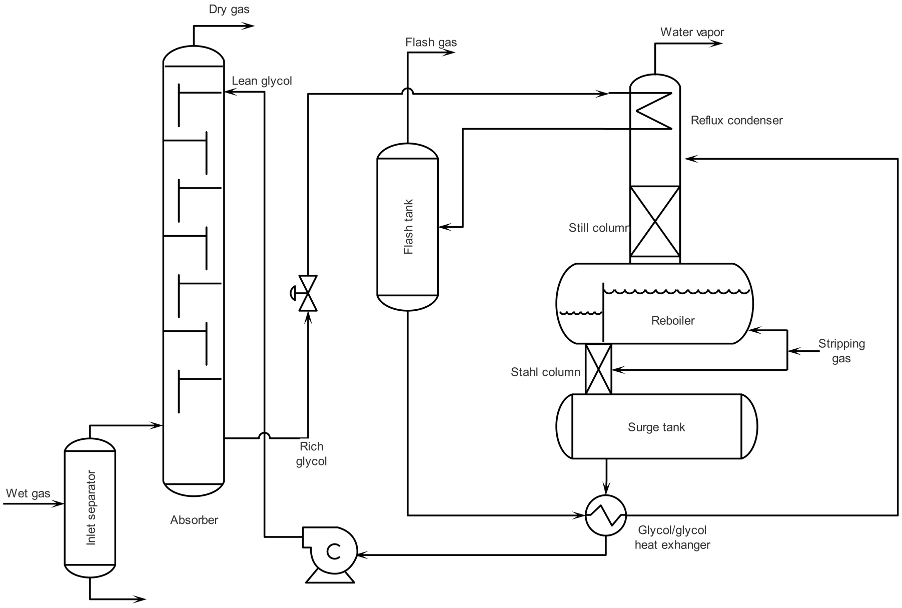

Figure 3.2: Process flow diagram of a gas dehydration process with injection of stripping gas for glycol regeneration

The stripping gas can be any inert gas, a part of the dehydrated gas or a fraction of the fuel gas. A basic scheme of the stripping gas injection process is presented in Figure 3.2.

3.2.2 Coldfinger water exhauster

The Coldfinger, also known as the Coldfinger water exhauster, is represented in Figure 3.3. It consists of a cold U-pipe (cold "finger") placed in the vapor space of a closed vessel containing the TEG mixture in vapor-liquid equilibrium coming from the regeneration column. Such vessel can be either a separate equipment, like the surge tank, or an integrated section of the reboiler. Through the inside of the pipe flows a cooling fluid that generally is the rich TEG coming from the absorber, and right under the coldfinger there is a tray for collection of the condensed vapor.

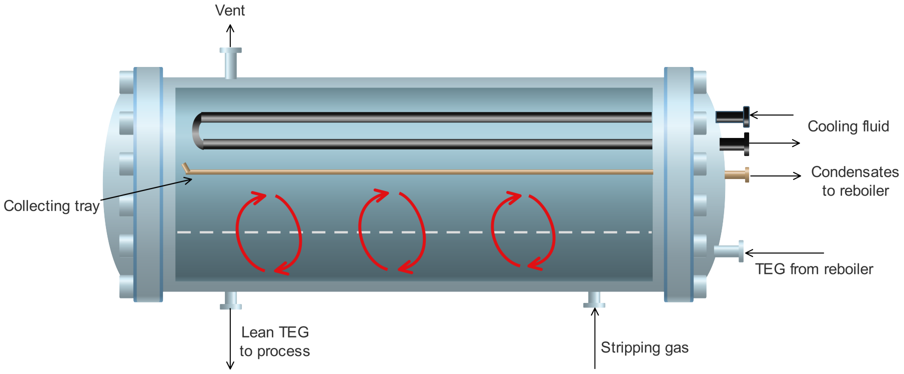

Figure 3.3: Schematic representation of the Coldfinger water exhauster

Normal operating conditions of the reboiler are 204 °C and atmospheric pressure therefore, TEG is a water-saturated liquid at such conditions. In order to obtain TEG at higher concentrations, it is necessary to shift the equilibrium conditions, which is accomplished by changing the overall composition of the system with the injection of small quantities of dry gas. Once the new state is achieved, some vapor will condense on the proximity of the cold pipe, accumulate on the collection tray and flow out of the equipment. By doing so, the equilibrium state of the mixture is upset, forcing the liquid at the bottom of the equipment to vaporize to reach a new equilibrium, removing more water from the liquid [10].

Moreover, the cold pipe located in the vapor space generates a temperature gradient inside the vessel, which is the driving force for the natural convection that will cause the internal recirculation of the uncondensed vapor to the bulk of the liquid. Since the uncondensed vapor remaining in the equipment is mainly dry gas, such recirculation will further enhance water exhaust from TEG [3]. Depending on the condensation needed, the cooling fluid is normally rich TEG leaving the absorption process but it can also be a coolant external to the process [10]. This unique method allows an increase of TEG concentration with small amounts of injected dry gas, making it an attractive alternative for enhanced TEG regeneration.
Figure 3.4 shows the process flow diagram of a gas dehydration unit with the Coldfinger water exhauster in the regeneration stage of glycol.

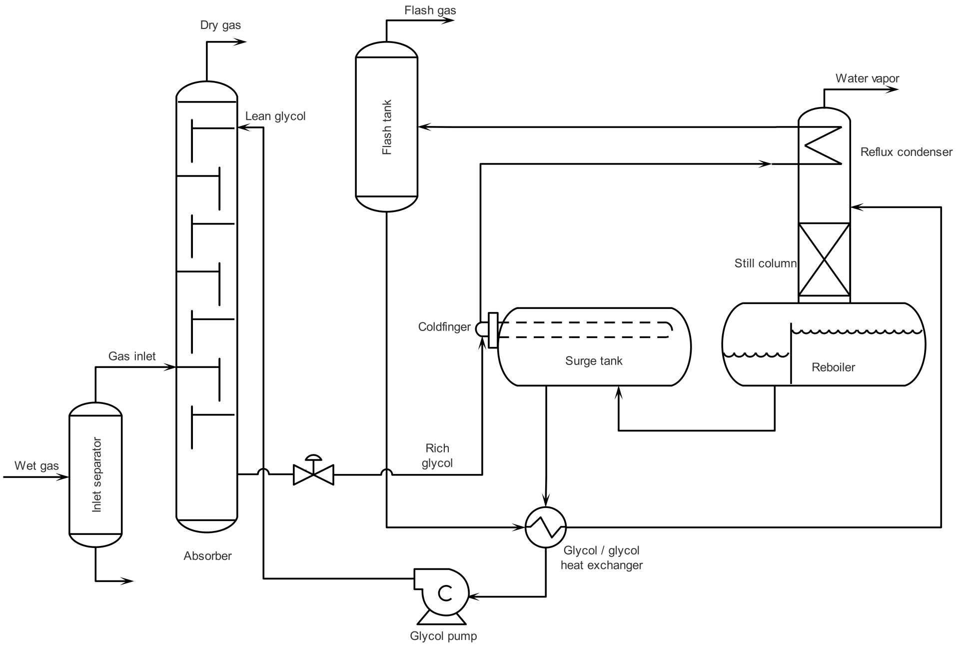

Figure 3.4: Process flow diagram of a gas dehydration process with Coldfinger water exhauster for the glycol regeneration process

3.3 Glycol-Water Equilibrium

At the operating conditions of the reboiler (low pressure, high temperature), it is possible to assume that the vapor phase behaves as an ideal gas thus, the vapor-liquid equilibrium conditions can be described by Raoult's Law, which is expressed in Equation 3.1:

$$y_i P = x_i P_{s_i}(T) \qquad (i = 1, 2, ...c) \tag{3.1}$$

Where y_i is the mole fraction of component *i* in the vapor, x_i is the mole fraction of component *i* in the liquid phase, P is the pressure of the system and $P_{s_i(T)}$ is the saturation pressure of component i at temperature T. The product y_iP is the partial pressure of component i. For water, Equation 3.1 results in:

$$x_w = \frac{y_w P}{P_{s_w}(T)} \tag{3.2}$$

The objective of the regeneration process is to minimize x_w. P_{s_w} is dependent on the system temperature; therefore, its value is set at the maximum allowable temperature at the reboiler. Finally, either the value of P or y_w have to be reduced in order to decrease x_w. When stripping gas is added to the reboiler, the composition of the vapor phase will change due to the addition of other components; consequently, the mole fraction of water in the vapor (y_w) will be reduced. On the other hand, pressure of the reboiler can be reduced by implementing a vacuum pump or an ejector [7].

Rearranging Equation 3.1 for y_i:

$$y_i = x_i \frac{P_{si}(T)}{P} \tag{3.3}$$

Similarly, based on Equation 3.3, it is possible to overview the behavior of the absorption process. Since the absorber operates at constant temperature, the ratio $P_{si}(T)/P$ is constant; thus, the concentration of water in the vapor is directly proportional to its concentration in the liquid phase. Even though the concentration of the liquid glycol is constantly changing as it flows down through the absorber, the counter-current flow operation allows a high transfer of water from the vapor to the liquid glycol and approach equilibrium [5].

3.4 Flash Calculations

The flash calculation is an important application of vapor-liquid equilibrium (VLE). The partial vaporization of a liquid is also called *flash* and occurs when the pressure of a liquid that is at a pressure equal to or greater than its bubble point pressure, decreases. Product of the pressure change is a two-phase system of vapor and liquid in equilibrium, with the vapor richer in the more volatile components [11].

Gibbs Phase Rule

The Gibbs phase rule defines the number of intensive variables or degrees of freedom (among temperature, pressure and composition), that must be fixed in order to specify the state of any system at equilibrium. It is expressed in Equation 3.4 [11]

$$DF = c + 2 - p \tag{3.4}$$

Where, DF is the degrees of freedom, c is the number of components present in the system and p is the number of phases.

The state of a system at equilibrium is defined when the temperature, pressure and composition of all phases are specified. For instance, a pure component ($c = 1$) in vapor-liquid equilibrium ($p = 2$) at certain pressure will have **one** independent variable ($DF = 1 + 2 - 2$), meaning that it can only exist in equilibrium at a defined pressure and temperature.

Phase-equilibrium calculations involve dependencies among intensive (quantity independent) and extensive (quantity dependent) variables. In this way, when some variables are defined, all other variables become fixed.

3.4.1 PT-flash calculations

PT-flash is one type of flash calculation and refers to the determination of the composition and relative amount of the vapor and liquid phases comprising a two-phase system in equilibrium at specified pressure, temperature and overall composition.

Considering a system of *c* components in vapor-liquid equilibrium, with overall composition z_i, α_v moles of vapor, x_i liquid mole fractions and y_i vapor mole fractions, the mass balance will be comprised of c equations of the form stated in Equation 3.5

$$z_i = x_i(1-\alpha_v) + y_i\alpha_v \qquad (i = 1, 2, ...c) \tag{3.5}$$

An important parameter in vapor-liquid equilibrium is the *K-value*, or equilibrium ratio, which measures the tendency of a component to go to the vapor phase or the liquid phase. It is defined in Equation 3.6

$$K_i \equiv \frac{y_i}{x_i} \qquad (i = 1, 2, ...c) \tag{3.6}$$

The *K-values* for Raoult's law, Equation 3.1, can be expressed as in Equation 3.7

$$y_i = K_i x_i \qquad (i = 1, 2, ...c) \tag{3.7}$$

Therefore, Equation 3.5 can be re-written considering the *K-values* as follows:

$$z_i = \alpha_v K_i x_i + (1-\alpha_v)x_i \qquad (i = 1, 2, ...c) \tag{3.8}$$

Solving Equation 3.8 for x_i and y_i :

$$x_i = \frac{z_i}{\alpha_v K_i + (1-\alpha_v)} \qquad (i = 1, 2, ...c) \tag{3.9}$$

$$y_i = \frac{K_i z_i}{\alpha_v K_i + (1-\alpha_v)} \qquad (i = 1, 2, ...c) \tag{3.10}$$

Considering the constraint on the mole fractions, represented in Equation 3.11:

$$\sum_{i=1}^{c}(y_i - x_i) = 0 \tag{3.11}$$

Finally, substituting Equation 3.11 in Equations 3.9 and 3.10:

$$\sum_{i=1}^{c}\frac{z_i(K_i-1)}{\alpha_v K_i + (1-\alpha_v)} = 0 \tag{3.12}$$

Equation 3.12 is known as the *Rachford-Rice equation*. By knowing the temperature, pressure and overall composition of the system, it is possible to solve Equation 3.12 for α_v finding in this way, a first approximation of the relative amounts of each phase and a first approximation of x_i and y_i as well.

Vapor-liquid equilibrium is met when the *isofugacity condition* is fulfilled, meaning that the fugacity of each species in all the phases is the same, as expressed in Equation 3.13:

$$f_i^v = f_i^l \qquad (i = 1, 2, ...c) \tag{3.13}$$

Introducing the concept of *fugacity coefficient* ($\phi_i = f_i/P$), Equation 3.13 is expressed as:

$$y_i P \phi_i^v = x_i P \phi_i^l \qquad (i = 1, 2, ...c) \tag{3.14}$$

Therefore, the *K-values* can be expressed as a function of the fugacity coefficients, as in Equation 3.15

$$K_i = \frac{\phi_i^l}{\phi_i^v} \qquad (i = 1, 2, ...c) \tag{3.15}$$

In this way, solving PT-flash calculations relies on calculating the fugacity coefficient of each species. Since ϕ_i^v is a function of pressure, temperature and y_i and ϕ_i^l is a function of pressure, temperature and x_i, the determination of the *K-values* necessary to determine the VLE requires, inevitably, an iterative process [11].

The iterative procedure to find the *K-values* is summarized in Figure 3.5.

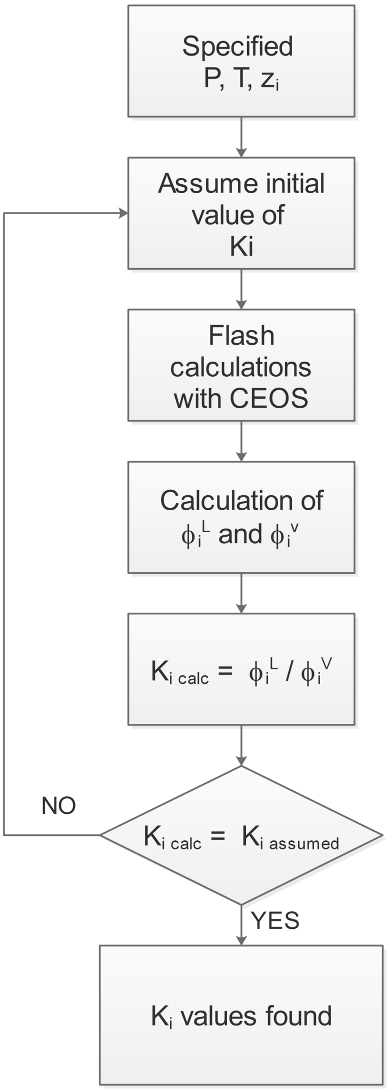

Figure 3.5: Flowchart for determining the *K-values* for flash calculations

Once the *K-values* are determined, the relative amount of the phases and its composition are defined.

3.5 Cubic Equations of State

Cubic equations of state are the simplest equations able to represent the behavior of the liquid and vapor phase. They consist of polynomial equations that are cubic in molar volume, making them general enough for their application in a wide range of temperatures and pressures [11].

Most equations are variations of the classic van der Waals equation of state, expressed in Equation 3.16:

$$P = \frac{RT}{V - b} - \frac{a}{V^2} \tag{3.16}$$

Where the term a, the attractive constant, and the term b, the covolume, are fluid-dependent parameters.

3.5.1 Peng-Robinson Equation of State

The Peng-Robinson equation of state is based on the van der Waals equation and is expressed in Equation 3.17:

$$P = \frac{RT}{\underline{V} - b} - \frac{a(T)}{\underline{V}(\underline{V} + b) + b(\underline{V} - b)} \tag{3.17}$$

Where P is the pressure, T is the temperature, $\underline{V}$ is the molar volume and R is the ideal gas constant.
In a mixture, the term $a(T)$ is dependent on temperature and composition, while the term b is dependent on composition, both determined at the critical conditions of temperature and pressure of the mixture, with the following expressions:

$$a_i(T) = \left(0.45724\frac{R^2T_c^2}{P_c}\right)\alpha(T) \tag{3.18}$$

$$b_i = 0.077780\frac{RT_c}{P_c} \tag{3.19}$$

Where, T_c and P_c are the critical temperature and pressure, respectively. The term $\alpha(T)$ is dependent on temperature and is a factor that ensures the correct prediction of the vapor pressure of the mixture through the cubic equation of state [12]. α(T) is expressed in Equation 3.20.

Moreover, according to the theorem of corresponding states, the compressibility factor of fluids compared at the same reduced pressure ($P_r = P/P_c$) and reduced temperature ($P_r = T/T_c$) exhibits similar behavior; however, deviations are observed for complex fluids. Thus, an empirical parameter, called *acentric factor (ω)*, is introduced to extend the validity of the theorem. In this way, $\alpha(T)$ is expressed as in Equation 3.20.

$$\alpha(T) = [1 + \kappa(1 - \sqrt{T/T_c})]^2 \tag{3.20}$$

$$\kappa = 0.37464 + 1.54226\omega - 0.26992\omega^2 \tag{3.21}$$

The acentric factor ω is characteristic of the molecular structure and is calculated for any fluid from T_c, P_c and a value of vapor pressure determined at $T_r = 0.7$ [11].

The dimensionless form of the Peng-Robinson equation of state is expressed in Equation 3.22:

$$z^3 + (-1 + B)z^2 + (A - 3B^2 - 2B)z + (-AB + B^2 + B^3) = 0 \tag{3.22}$$

where

$$A = \frac{a(T)P}{(RT)^2} \tag{3.23}$$

$$B = \frac{bP}{RT} \tag{3.24}$$

Consequently, the equation of state for pure components is completely defined once the critical pressure, critical temperature and acentric factor are known.
Additionally, for the accurate prediction of the phase behavior of mixtures by using equations of state, it is necessary to account for their dependence on the mixture composition [12]. As stated before, the fluid-dependent parameters for a mixture *a(T)* and b depend on composition; nevertheless, there is not an established theoretical description of such dependence. Instead, empirical *mixing rules* have been established to relate the mixture parameters to the ones for pure components [11].

The simplest expressions are the ***van der Waals mixing rules***, shown in Equations 3.25 and 3.26:

$$a = \sum_{i=1}^{c}\sum_{j=1}^{c}(x_i x_j a_{ij}) \tag{3.25}$$

with $a_{ii} = a_i$ and $a_{ij} = \sqrt{a_i a_j}(1 - k_{ij})$

$$b = \sum_{i=1}^{c}\sum_{j=1}^{c}(x_i x_j b_{ij}) \tag{3.26}$$

with $b_{ii} = b_i$ and $b_{ij} = \frac{b_i + b_j}{2}(1 - \eta_{ij})$

The terms k_{ij} and η_{ij} are the *binary interaction parameters* and are obtained by fitting predictions from the cubic equation of state to measured values of phase equilibrium [12].

3.5.2 CEOS in Commercial Process Simulators

The commercial process simulator widely used in the oil and gas industry is Aspen HYSYS®; therefore, the analysis is based on this simulator.

Aspen HYSYS® has an extensive library of equations of state, named *Property Packages*, available for building a simulation case. Two of these are the Peng-Robinson and the Glycol Property Package.

Peng-Robinson Property Package

The Peng-Robinson property package is based on the Peng-Robinson equation of state, which is the same defined in Equation 3.17. The dimensionless form used by the Peng-Robinson porperty package is the following [13] :

$$z^3 + (1 - B)z^2 + (A - 2B - 3B^2)z - (AB - B^2 - B^3) = 0 \tag{3.27}$$

where:

$$b = \sum_{i=1}^{N}(x_i b_i)$$

$$b_i = 0.077796\frac{RT_{ci}}{P_{ci}}$$

$$a = \sum_{i=1}^{N}\sum_{j=1}^{N} x_i x_j (a_i a_j)^{0.5}(1 - k_{ij})$$

$$a_i = a_{c_i}\alpha_i$$

$$a_{c_i} = 0.457235\frac{R^2 T_{c_i}^2}{P_{c_i}}$$

$$\alpha_i^{0.5} = 1 + m_i(1 - \sqrt{T/T_{c_i}})$$

$$m_i = 0.37464 + 1.54226\omega_i - 0.26992\omega_i^2 \tag{3.28}$$

When $\omega_i > 0.49$ the following form for m$_i$ is considered:

$$m_i = 0.379642 + (1.48503 - (0.164423 - 0.016666\omega_i)\omega_i)\omega_i \tag{3.29}$$

$$A = \frac{aP}{(RT)^2}$$

$$B = \frac{bP}{RT}$$

The equation of state used in Aspen HYSYS® corresponds to the improved version of the Peng Robinson EOS developed in 1978 by the same authors [14] which considers an additional κ function for acentric factors different to 0.49. Additionally, the expression for the covolume (b) does not take into account the binary interaction parameter η_{ij}, differing from its original expression.

Glycol Property Package

Aspen HYSYS® is provided with the Glycol property package, which has been developed for modeling glycol dehydration processes using TEG by representing the phase behavior of the TEG-water binary system in a more accurate way. This property package is based on the Twu-Sim-Tassone (TST) equation of state and contains the necessary binary interaction parameters for the typical components encountered in a natural gas dehydration process [13].

The Glycol property package is applicable for gas dehydrator temperatures between 15 °C to 50 °C and pressures between 10 atm (1 MPa) to 100 atm (10 MPa) and for glycol regenerator temperatures between 202 °C to 206 °C and 1.2 atm (0.12 MPa) [13].
The TST cubic equation of state is stated in Equation 3.30:

$$P = \frac{RT}{v - b} - \frac{a}{(v + 3b)(v - 0.5b)} \tag{3.30}$$

Where v is the molar volume and a, b are the cubic equation of state parameters obtained at the critical point. a and b are expressed as follows:

$$a_c = 0.470507\frac{R^2T_c^2}{P_c}$$

$$b_c = 0.0740740\frac{RT_c}{P_c}$$

Since the parameter *a* is a function of temperature, the value of a(T) at temperatures other than the critical temperature is calculated with Equation 3.31

$$a(T) = \alpha(T)a_c \tag{3.31}$$

$$\alpha(T) = T_r^{N(M-1)}e^{L(1-T_r^{NM})} \tag{3.32}$$

L, M and N are parameters inherent for each component [13].

The parameters a and b of the TST EOS for mixtures are defined through the zero-pressure mixing rules, which accounts for the excess Helmholtz energies at zero pressure [13].

3.6 Energy Balance

Energy conservation is expressed through an energy balance equation, where the energy rate of change of a system equals the net energy rate transferred into the system in the form of heat, work and energy transported by flowing streams [11].
Flowing streams entering and exiting an open system have associated with them internal, potential and kinetic energy, all contributing to the total energy change of the system. In this way, the total energy carried by a mass of flowing stream is $(U + 1/2v^2 + gh)$, and the rate of energy transported is $(U + 1/2v^2 + gh)\dot{m}$.

Work may be present in several forms. One of them is the work exerted by streams entering and leaving the system, expressed as $(\dot{m}PV)$. Another form is deformation work, which is the work associated with the force exerted by the surrounding pressure on the system causing movement of the system boundaries, expressed as $-P\frac{\mathrm{d}V}{\mathrm{d}t}$. The other form of work is the shaft work, which is the energy exchanged by the system due to interactions with moving parts of the surroundings, like impellers, without causing movement of the system boundaries. The shaft work is expressed as $\dot{W}_s$.
Thus, the general energy balance for an open system is:

$$\frac{\mathrm{d}E_T}{\mathrm{d}t} = \dot{Q} - P\frac{\mathrm{d}V}{\mathrm{d}t} + \dot{W}_s + \sum\left[\dot{m}\Big(\hat{U} + \frac{v^2}{2} + gh\Big) + \dot{m}P\hat{V}\right]$$

Knowing that enthalpy H is defined as $U + PV$, where U is the internal energy, then the energy balance equation can be rewritten to the form stated in Equation 3.33:

$$\frac{\mathrm{d}E_T}{\mathrm{d}t} = \dot{Q} - P\frac{\mathrm{d}V}{\mathrm{d}t} + \dot{W}_s + \sum\left[\dot{m}\Big(\hat{H} + \frac{v^2}{2} + gh\Big)\right] \tag{3.33}$$

In most chemical engineering applications, kinetic and potential energy are negligible[11], leading to the final form of the energy balance, stated in Equation 3.34

$$\frac{\mathrm{d}U}{\mathrm{d}t} = \dot{Q} - P\frac{\mathrm{d}V}{\mathrm{d}t} + \dot{W}_s + \sum(\dot{m}\hat{H}) \tag{3.34}$$

4 State of the Art

The Coldfinger was first disclosed in 1971 as an apparatus for dehydrating organic liquids miscible with water [15]. Later, in 1982 this technology was introduced as part of a methodology for removing water from glycol solutions [10]. Since then, only few studies report models for the Coldfinger unit for natural gas dehydration.

For instance, Gironi et al. [3] modeled the Coldfinger apparatus by means of a user-defined external routine, later annexed to the simulation of a natural gas dehydration plant and studied the influence of the most relevant operating parameters on the performance of the water exhauster. However, this work does neither report an in-depth analysis of the influence of the temperature at the upper section of the water exhauster, nor considers the injection of dry gas in the bottom section of the equipment, which is found in real regeneration processes.

Additionally, Øi and Selstø [16] reported a strategy for modeling the Coldfinger in the commercial process simulator Aspen HYSYS®, but they did not provide a model of the equipment based on its physical principles. Moreover, in their work, an energy stream (heat) was added to the Coldfinger instead of stripping gas to perform the equilibrium calculations, which is not seen in real applications.

Finally, Rahimpour et al. [17] presented a methodology for modeling the Coldfinger based on a heat transfer approach, by iteration of the outlet temperature of the cooling fluid through the Coldfinger tubes, together with element-wise equilibrium calculations along the exhauster with local balances in each element. Even though the parameter study considered stripping gas flow rate, it did not consider the effect of the variation of temperature at the upper section of the apparatus nor the stripping gas-TEG ratio influence on the performance of the water exhauster in a glycol regeneration process.

5 Methodology

In this project, the Coldfinger water exhauster is modeled considering phase equilibrium and the internal recirculation of the vapor inside the equipment. The conceptual modeling of the Coldfinger is carried out through self-developed routines in Matlab, while the analysis of the behavior of the proposed conceptualization in a gas dehydration process is developed in the commercial process simulator Aspen HYSYS® V9.

5.1 Conceptualization

Considering the description of the water exhauster stated in Section 3.2.2, the Coldfinger is modeled as two contiguous compartments where two-stage phase equilibrium takes place, as represented in Figure 5.1

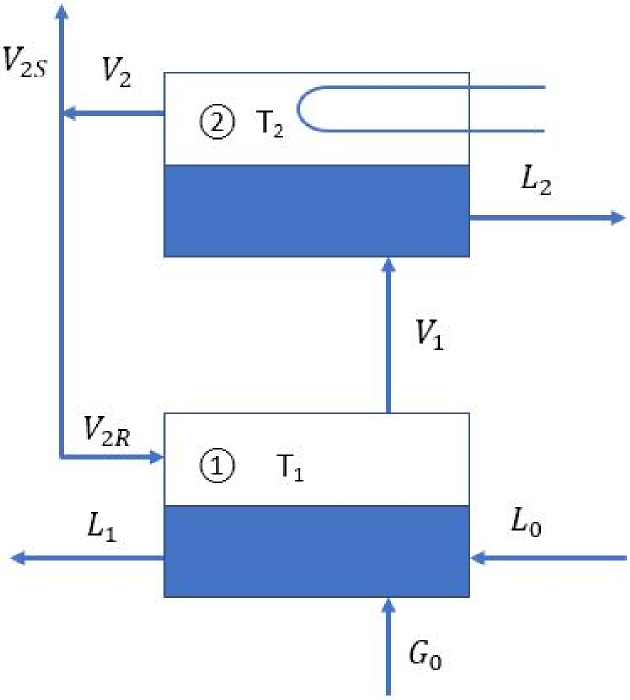

Figure 5.1: Conceptual model of the Coldfinger water exhauster

The first compartment (bottom section) contains the enhanced regenerated TEG (L_1) in equilibrium with its vapor (V_1) due to the constant injection of stripping gas (G_0) to the liquid stream coming from the reboiler (L_0).

The second compartment (top section) receives the vapor coming from the bottom section (V_1), which is partially condensed due to the temperature drop caused by the cold fingers. The liquid condensed on the surface of the cooling pipe and removed from the vessel (L_2) is in equilibrium with the uncondensed vapor (V_2). The natural convection is here represented by considering a continuous reflux of a certain amount of the vapor generated in the second compartment to the first one (V_{2R}). The remaining vapor (V_{2S}) is vented upstream the water exhauster.

The conceptual study is performed considering pure methane as the stripping gas injected at the bottom section and a binary mixture of water-TEG coming from the reboiler, thus obtaining a three-component system inside the Coldfinger formed by methane(1) – water(2) – TEG(3).

Although the dry gas available in dehydration units is not pure methane and the liquid stream coming from the reboiler contains also traces of other chemical species, the components other than the three reported above are present in small amount; therefore, they are neglected in this conceptual study. Additionally, the temperature drop of the bottom section caused by the mixing of the recirculated uncondensed vapor is neglected, and the temperature of the bottom section is fixed at the same temperature of the reboiler (204°C).

The conceptual study focuses on the effect of the temperature at the top section of the Coldfinger, which depends on the heat power removed from the system and on the internal recirculation, which depends on the temperature difference between the two sections of the equipment and on its design.

5.2 Thermodynamic Model

The thermodynamic model used for the Coldfinger water exhauster is based on the Peng-Robinson equation of state (EOS) and the classic form of the quadratic mixing rules (van der Waals mixing rules). The critical parameters and acentric factor of the three components of the system under study are shown in Table 5.1
Data for methane are taken from Perry (1999), whereas data for water and TEG are taken from Gironi et al. (2010).

Table 5.1: Critical parameters and acentric factors for methane, water and TEG

Component	Pc, MPa	Tc, K	Acentric factor	Reference
Methane, CH_4	4.59	190.564	0.011	[18]
Water, H_2O	22.12	647.3	0.344	[19]
Triethylene glycol, TEG	3.958	806.3	0.563	[19]

The binary interaction parameters (k_{12}) were taken or regressed from available literature data. Gironi et al. [19, 20] reported a linear relation of k_{12} with respect to temperature for the TEG-water binary system, which is used in this work, and stated in Equation 5.1:

$$k_{ij}(T) = 0.000482T - 0.3935 \tag{5.1}$$

For the CH_4-TEG and CH_4-H_2O binary systems, the binary interaction parameters were obtained by regression of experimental data of solubility of CH_4 reported in previous works, considering the minimization of the objective function (ϕ) presented in Equation 5.2:

$$\phi = \sum_{i=1}^{N} (x_{exp} - x_{calc})_i^2 \tag{5.2}$$

where, x_{exp} and x_{calc} are the experimental and calculated mole fractions of CH_4 in the liquid phase, respectively; the subscript i stands for the i-th experimental data, while N represents the total number of experimental data.

5.2.1 Binary interaction parameters for the system CH_4-TEG

In previous works developed by Jou et al. [21], the solubility of light alkanes, among them methane, in triethylene glycol was determined for different values of temperature ranging from 298.15 to 398.15 K and ten different values pressure ranging from 0.1 to 20 MPa for each value of temperature under analysis. The T-P-x experimental values reported for the system TEG(1)-CH_4(2) were used for obtaining the binary interaction parameter (BIP) at which Equation 5.2 presented the minimum value, for each value of temperature. These results are presented in Table 5.2.

Table 5.2: Objective function values and their corresponding BIP for the system TEG-CH_4

Temperature, K	k_{ij}	ϕ_{min}
298.15	0.2071	1.02×10^{-5}
325.15	0.2139	2.79×10^{-6}
348.15	0.2221	4.90×10^{-7}
373.15	0.2285	6.36×10^{-7}
398.15	0.2313	3.19×10^{-7}

With the values reported in Table 5.2, the regression of the binary interaction parameter as function of temperature was performed, obtaining the results presented in Figure 5.2

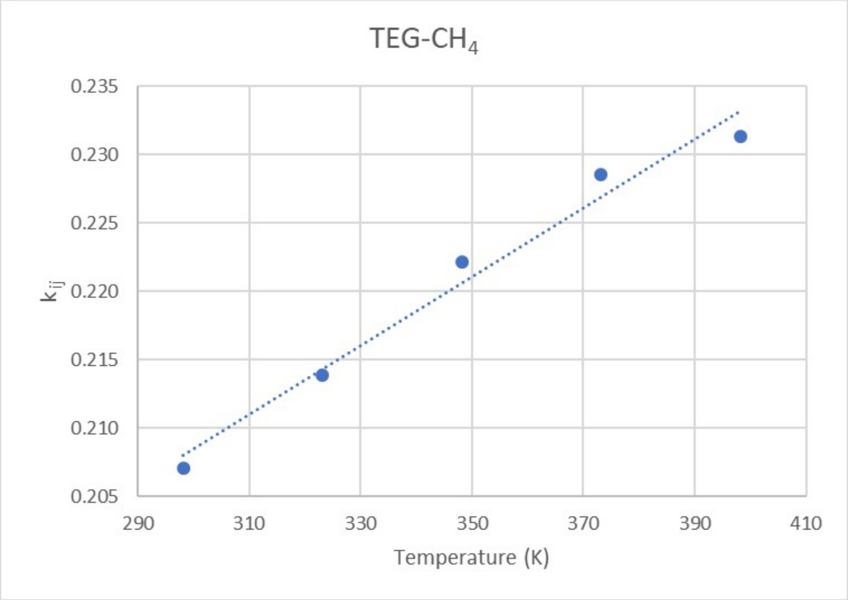

Figure 5.2: BIP regression from experimental data, system TEG-CH_4

With the above data, a linear relation of k_{ij} with temperature was obtained for this system, expressed in Equation 5.3.

$$k_{ij}(T) = 0.00030T + 0.1328 \tag{5.3}$$

The average absolute deviation (AAD) between the experimental and calculated data using the function of Equation 5.3 is 2.09×10^{-3}.

5.2.2 Binary interaction parameters for the system CH_4-H_2O

A similar approach was developed for the system CH_4-H_2O. In previous works developed by Coulberson and McKetta [22], the solubility of methane in water was determined for different values of temperature ranging from 298.15 to 410.93 K and 14 values of pressure ranging from 1 to 69 MPa for each value of temperature under analysis. The T-P-x experimental values reported for the system CH_4-H_2O were used for obtaining the binary interaction parameter (BIP) at which Equation 5.2 presented the minimum value, for each value of temperature. These results are presented in Table 5.3.

Table 5.3: Objective function values and their corresponding BIP for the system CH_4-H_2O

Temperature, K	kij	ϕ_{min}
298.15	-0.3082	1.97×10^{-9}
310.93	-0.2720	6.69×10^{-9}
344.26	-0.1792	5.37×10^{-9}
377.59	-0.0985	2.95×10^{-9}
410.93	-0.0270	7.48×10^{-9}

With the values reported in Table 5.3, the regression of the binary interaction parameter as function of temperature was performed, obtaining the results presented in Figure 5.3

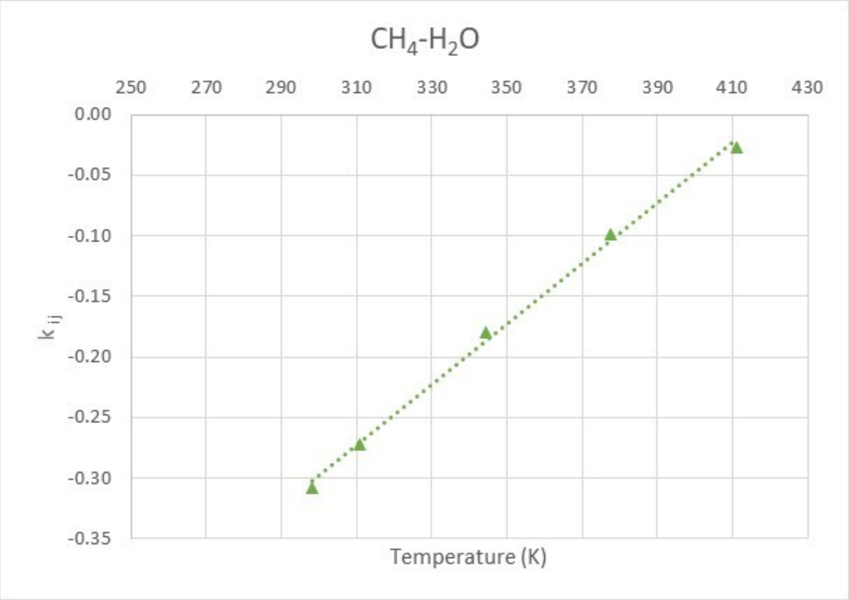

Figure 5.3: BIP regression from experimental data, system TEG-CH_4

With the above data, a linear relation of k_{ij} with temperature was obtained for this system, expressed in Equation 5.4.

$$k_{ij}(T) = 0.00251T - 1.05038 \tag{5.4}$$

The average absolute deviation (AAD) between the experimental and calculated data using the function of Equation 5.4 is 8.47×10^{-5}.

5.3 Matlab Modeling

The Coldfinger water exhauster was modeled considering two main parameters: internal vapor recirculation ratio, α, and gas-to-liquid feed ratio, β, defined in Equations 5.5 and 5.6, respectively.

$$\alpha = \frac{V_{2R}}{V_2} \tag{5.5}$$

$$\beta = \frac{G_0}{L_0} \tag{5.6}$$

The input parameters for the model are shown in Table 5.4:

Table 5.4: Coldfinger modeling input parameters for the system CH_4 (1) – H_2O (2) - TEG (3)

Parameter	Value	Unit
Operating pressure, P	101.325	kPa
Bottom section temperature, T_1	204	°C
Top section temperature, T_2	34 to 204	°C
Composition of liquid from reboiler, x_0	x_{1_0}=0 x_{2_0}=0.0771 x_{3_0}=0.9229	mole fraction
Composition of stripping gas, y_0	y_{1_0}=1	mole fraction
Internal vapor recirculation ratio, α	0 to 0.99	-
Gas-to-feed liquid ratio, β	1×10^{-6} to 1×10^{-2}	-

The subscript convention adopted for a better management of the Matlab model and its results considers two subscripts ranging from 0 to 2 and from 1 to 2 each. The first subscript stands for the *component* and the second subscript for the *location*. Component refers to CH_4 (subscript 1), H_2O (subscript 2) and TEG (subscript 3) whereas location refers to inlet stream (subscript 0), bottom section (subscript 1) and top section (subscript 2). For example, $\mathbf{x}_{3_1}$ refers to the value of component 3 (TEG) in the bottom section (1).

The internal vapor recirculation ratio, α, considered in the analysis was varied on five levels: 0, 0.3, 0.5, 0.8 and 0.99; the last value is intended to reproduce the behavior of the Coldfinger when nearly all the vapor of the top section recirculates to the bottom . On the other hand, the **base case** of analysis corresponds to $\alpha = 0$, where no vapor from the top section recirculates to the bottom section, representing a conventional single-stage stripping process.

Additionally, the gas-to-liquid feed ratio, β, was varied from 0.0001 to 0.01 with variations of 0.0015. The value of β of 1×10^{-6}, i.e. stripping gas injection tends to zero, is intended to reproduce the behavior of the Coldfinger when there is no injection of stripping gas.

Finally, T_2 was varied from 204 °C, equivalent to no heat removal in the top section, down to 34 °C. The minimum temperature is consistent with the use of cold water as an external cooling agent through the Coldfinger.

The Matlab routine for modeling the Coldfinger water exhauster is summarized in Figure 5.4.

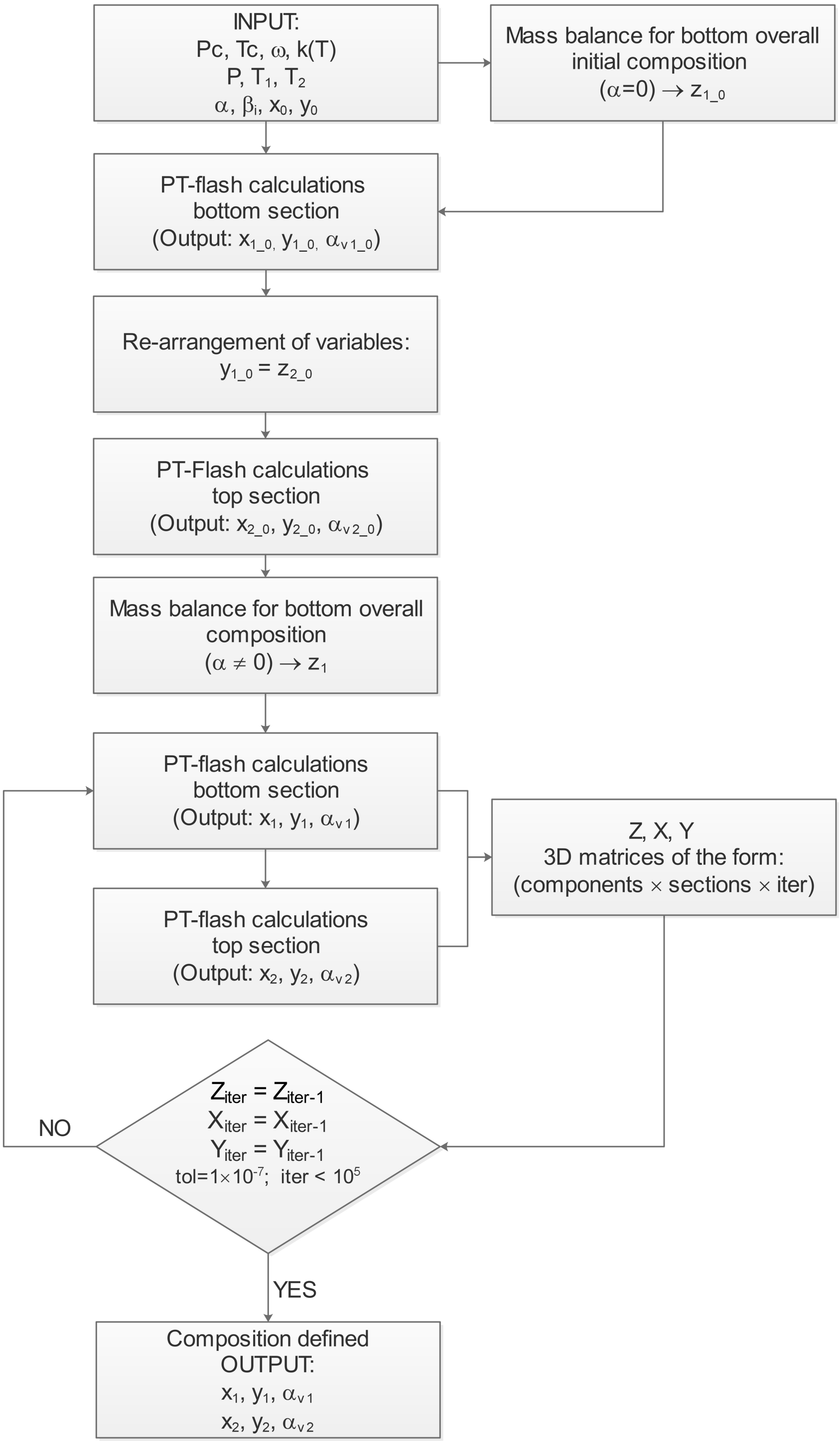

Figure 5.4: Routine for modeling the Coldfinger process in Matlab

The sequence of continuous PT-flash calculations are performed for a fixed value of recirculation ratio and all the values of top section temperature per value of gas-to-liquid ratio defined in the corresponding inlet vector. Once convergence is achieved for the selected value of α, a next value is defined and the sequence repeated for all the values of the vector β.

As it can be seen in Figure 5.4, the modeling process starts by estimating the overall composition of the bottom section. In an initial stage, the equipment contains the saturated liquid coming from the reboiler; since there is still no injection of stripping gas, there is not vapor-liquid equilibrium and thus, no vapor is recirculated to the bottom section yet. As stripping gas is considered, the overall composition of the bottom section will change from a two-component (H_2O-TEG) to a three-component mixture (CH_4-H_2O-TEG); therefore, a mass balance is applied to the bottom section in order to define its initial overall composition. Once such composition is determined, PT-flash calculations are applied to the bottom section of the equipment in order to define the composition of the liquid and vapor in co-existing equilibrium.

The conceptual study considers that all the vapor in equilibrium with the liquid of the bottom section enters in contact with the cooling pipe of the top section. Thus, a re-arrengement of variables is done before determining the equilibrium composition of the top section. Consequently, the composition of the vapor of the bottom section is now considered as the overall initial composition of the top section and PT-flash calculation are applied.

Now that vapor can be recirculated to the bottom section, the recirculation ratio α, defined in the input parameters of the sequence, is taken into account to perform a new mass balance in the bottom section and define its new overall composition. Similarly, the re-arrangement of variables is considered and PT-flash calculation are applied to the top section.

The routine is developed considering a *While* loop, meaning that convergence criteria is defined for obtaining a solution. In other words, the calculation will continue until the convergence criteria is false. In this case, the evaluation is made considering a minimum difference between the composition of each phase of each section at the i^{th} calculation step and the composition of each phase phase of each section at the previous calculation step. If the criteria is met, then the composition of the co-existing phases for both sections are defined.

Finally, the effect of the temperature of the top section in the behavior of the Coldfinger is estimated through an energy balance in the top section.

5.4 Energy Balance

In this study, the bottom section of the Coldfinger water exhauster is considered at isothermal operating conditions, meaning that the temperature variation takes place in the top section of the vessel (second compartment). Therefore, energy balance calculations are applied to the top section of the Coldfinger.

Starting from the equation of the energy balance for open systems, stated in Equation 3.34, for a steady state process with no shaft work, it can be re-written as in Equation 5.7.

$$0 = \dot{Q} + \sum(\dot{m}\hat{H}) \tag{5.7}$$

Considering the second compartment of Figure 5.1, the open system from which heat power is exchanged by the system is represented in Figure 5.5.

Based on Figure 5.5 and on Equation 5.7, the energy balance for the Coldfinger water exhauster is:

$$\dot{Q} = V_2 H_{V_2} + L_2 H_{L_2} - V_1 H_{V_1} \tag{5.8}$$

Where $\dot{Q}$ is the heat power exchanged by the system, V_2 is the mass flow of vapor leaving the second compartment, H_{V_2} is its enthalpy, L_2 is the mass flow of liquid leaving the

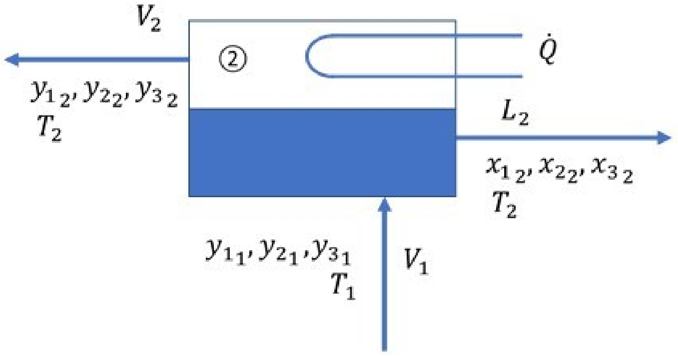

Figure 5.5: Open system diagram (Coldfinger second compartment) for energy balance

second compartment, H_{L_2} is its corresponding enthalpy, V_1 is the mass flow of vapor entering the second compartment and H_{L_2} is its enthalpy.

Expressing Equation 5.8 per unit mass flow of the liquid feed entering the Coldfinger water exhauster (L_0), leads to Equation 5.9 , used in this work to determine the specific heat removed from the system.

$$\frac{\dot{Q}}{L_0} = \frac{V_2}{L_0} H_{V_2} + \frac{L_2}{L_0} H_{L_2} - \frac{V_1}{L_0} H_{V_1} \tag{5.9}$$

Finally, a reference state was established to determine the specific heat removed from the system. For the ternary system CH_4-H_2O-TEG, the reference states are as follows:

- Water, pure liquid @ 204 °C
- TEG, pure liquid @ 204 °C
- CH_4, pure gas @ 204 °C

The expression for determining the latent heat of vaporization, heat capacity of liquid and heat capacity of vapor for the three components of the system were taken from Yaws [23], as follows:

Latent heat of vaporization

$$H_{vap} = A\left(1 - \frac{T}{T_c}\right)^n \tag{5.10}$$

Where, H_{vap} is expressed in $\frac{kJ}{mol}$, T in K:

Component	A	n
Methane, CH_4	10.312	0.265
Water, H_2O	52.053	0.321
Triethylene Glycol, TEG	130.88	0.46

Heat capacity of liquid

$$Cp_L = A + BT + CT^2 + DT^3 \tag{5.11}$$

Where, Cp_L is expressed in $\frac{kJ}{molK}$, T in K:

Component	A	B	C	D
Water, H_2O	92.053	-3.9953$\times10^{-2}$	-2.1103$\times10^{-4}$	5.3469$\times10^{-7}$
Triethylene Glycol, TEG	162.2330	1.2720	-3.0443$\times10^{-3}$	2.9863$\times10^{-6}$

Heat capacity of vapor

$$Cp_V = A + BT + CT^2 + DT^3 + ET^4 \tag{5.12}$$

Where, Cp_V is expressed in $\frac{kJ}{molK}$, T in K:

Component	A	B	C	D	E
Methane, CH_4	34.942	-3.9957$\times10^{-2}$	1.9184$\times10^{-4}$	-1.5303$\times10^{-7}$	3.9321$\times10^{-11}$
Water, H_2O	33.933	-8.4186$\times10^{-3}$	2.9906$\times10^{-5}$	-1.7825$\times10^{-8}$	3.6934$\times10^{-12}$
Triethylene Glycol, TEG	2.1010	0.7865	-5.6060$\times10^{-4}$	2.0905$\times10^{-7}$	-3.3896$\times10^{-11}$

In this way, through Equations 5.10, 5.11 and 5.12 enthalpy can be expressed as a function of temperature with respect to the reference state, previously defined, taking into consideration the state of aggregation of each stream.

5.5 HYSYS® Modeling

The Coldfinger water exhauster was modeled in HYSYS® considering the conceptualization stated in section 5.1 of this report; thus, it was modeled with two two-phase flash separators to represent the bottom and top compartments; a heat exchanger to represent the heat removal from the top section; and a recycle stream of the vapor of the second flash separator to the first one to represent the natural convection. The general process diagram is represented in Figure 5.6

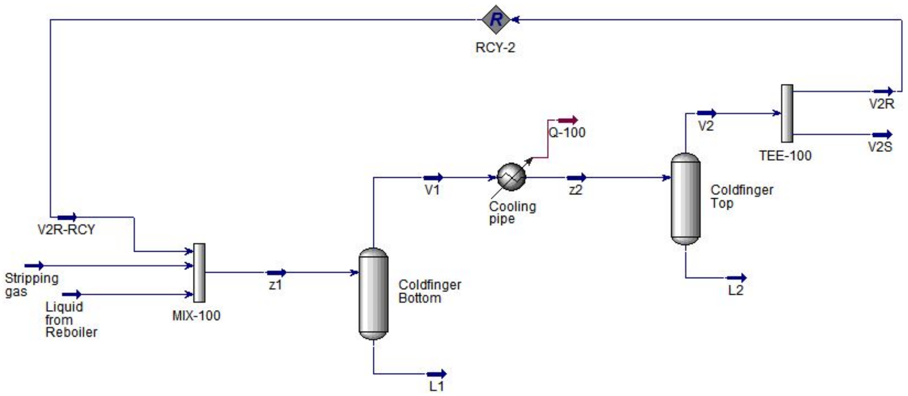

Figure 5.6: Process flow diagram of the Coldfinger water exhauster in HYSYS®

The main differences of this HYSYS® model with the one developed by Øi and Selstø [16], is the consideration of natural convection through the recirculation of a fraction of the vapor of the second flash separator to the first one, to analyze its influence on the performance of the Coldfinger, and the injection of stripping gas to the first flash separator; instead of the total vapor recirculation and the energy supply to the first flash separator considered by the mentioned authors.

The selection of the thermodynamic model is a critical aspect when building the HYSYS® simulation. It is necessary to identify the similarities and the differences of the thermodynamic model in the process simulator with the one defined in the conceptual model, to see if comparable results are possible to achieve. According to the information stated in section 3.5.2 of this report, the form of the Peng-Robinson equation of state used by HYSYS® when selecting the *Peng-Robinson Fluid Package* (3.17) is similar to the one used in the conceptual study of Coldfinger in Matlab. However, a significant difference relies in the equation for κ in the mixing rules used by the commercial simulator for the cases when $\omega > 0.49$ (Equation 3.29).

Another difference is the input option for the BIP in HYSYS®. When selecting the Peng-Robinson fluid package, the matrix accepts scalars as input, meaning that the value of the binary interaction parameters will remain constant during the process and will not vary with temperature, opposed to what is considered in the conceptual study.

Due to these differences, it is not possible to use the Peng-Robinson fluid package to build the simulation in the commercial process simulator and make a direct comparison with the results of the conceptual study. Thus, the HYSYS® simulation was built considering the *Glycol Fluid Package*, which is featured in the simulator for a better analysis of processes handling glycols.

First, the conceptualization of the water exhauster was build in HYSYS® with a three-component system formed by CH_4, H_2O and TEG, with the aim of analyzing the behavior of the conceptual model in the commercial process simulator. Then, the conceptual model is introduced in the simulation of a gas dehydration process in order to analyze its performance under real operating conditions with a multi-component system.
The values of critical parameters-acentric factors and binary interaction parameters set by default in this fluid package were used in the simulation, which are presented in Table 5.5 and Table 5.6, respectively.

Table 5.5: Critical parameters and acentric factors for pure components - Glycol Fluid Package

Component	Pc, MPa	Tc, °C / K	Acentric factor
Methane, CH_4	4.64068	-82.4510 / 190.7	0.011498
Water, H_2O	22.12	374.149 / 647.3	0.344
Triethylene Glycol, TEG	1.41855	453.850 / 727.0	0.68997

Table 5.6: Binary interaction parameters for the system CH_4-H_2O-TEG - Glycol Fluid Package

Pair	Binary interaction parameter
CH_4-H_2O	1.51875
CH_4-TEG	0
H_2O-TEG	0

Comparing the values presented in Table 5.5 with the ones of Table 5.1, it is seen that the major difference relies on the critical properties and acentric factor for TEG. Critical pressure and temperature for TEG in the Glycol package are lower than the ones considered for the Matlab model, while the corresponding acentric factor is higher in the Glycol package than in the Matlab model.

Once the Coldfinger conceptualization was analyzed with a three-component system, the gas dehydration process was built considering the conceptual model of the Coldfinger water exhauster for the regeneration process of TEG and the referential operating parameters of a gas dehydration unit with glycol presented in Table 3.3.
The composition of the wet gas stream entering the dehydration process is presented in Table 5.7.

Table 5.7: Wet gas composition

Component	molar fraction
Nitrogen	0.0080
CO_2	0.0010
Methane	0.5680
Ethane	0.1260
Propane	0.1500
i-Butane	0.0300
n-Butane	0.0760
i-Pentane	0.0150
n-Pentane	0.0160
n-Hexane	0.0060
H_2O	0.0040

The effect of the composition of the injected stripping gas into the Coldfinger was considered in the study; therefore, eight cases were built to analyze the behavior of the conceptual model of the Coldfinger water exhauster, considering either pure CH_4 or multi-component gas stream injection. The cases are described as follows:

Table 5.8: Study cases for the gas dehydration process with Coldfinger water exhauster

Case name	α	β	Stripping gas composition
Base case 1	0	0.001	100 % CH_4
Base case 2	0	0.001	Dry gas composition
Case 3	0.99	0.001	100 % CH_4
Case 4	0.99	0.001	Dry gas composition
Case 5	0.80	0.001	100 % CH_4
Case 6	0.80	0.001	Dry gas composition
Case 7	0	0.001	100 % CH_4
Case 8	0	0.001	Dry gas composition

Base cases (1 and 2) as stated in Table 5.8, correspond to the cases where the internal vapor recirculation ratio (α) is zero, representing single-stage stripping processes with pure methane and multi-component stripping gas, respectively. Cases 7 and 8 were built in order to determine the amount of stripping gas needed to reach a specific TEG purity using a single-stage stripping process ($\alpha = 0$) to further regenerate TEG, keeping the same gas-to-feed liquid ratio (β) as base of comparison.

6 Results

The selected binary interaction parameter for the system H_2O-TEG, Equation 5.1, along with the critical parameters and acentric factor considered in the conceptual model, gave as result a TEG concentration of 99 wt.% in the liquid stream coming from the reboiler at 204 °C and atmospheric pressure. This value represents the baseline of analysis of the Coldfinger performance.

6.1 Matlab Modeling Results

The conceptual study was developed considering a binary mixture H_2O-TEG coming from the reboiler and a ternary mixture CH_4-H_2O-TEG inside the equipment, after the injection of stripping gas. As a result of this study, it is possible to clearly see the enhanced TEG regeneration due to the Coldfinger, as compared to the base case (conventional stripping, $\alpha = 0$).

6.1.1 Effect of top temperature

The effect of the top temperature in the performance of the Coldfinger is shown in Figure 6.1, which shows the enhanced TEG purity obtained for the entire range of top temperature values under analysis, considering different values of stripping gas (β) and different values of internal vapor recirculation. It is seen that the purity of the enhanced regenerated TEG decreases as the temperature at the top section of the equipment increases.
In addition, the shape of the curves shows that the Coldfinger process is not efficient when there is only little cooling of the vapor in the top section. This behavior is reproduced for all the values of internal vapor recirculation considered, except for $\alpha = 0$ where the regenerated TEG purity remains constant and independent from T_2 due to the absence of vapor recirculation.

From Figure 6.1, it is also possible to observe the positive effect of the internal vapor recirculation on the improved regeneration of TEG. For a certain value of β, the purity of TEG increases as the value of α increases, obtaining a maximum reconcentration when α approaches the unity, i.e minimum venting. Figure 6.1 shows the results obtained when $\beta = 0.001$.

Another way to evaluate the effect of the temperature of the top section in the behavior of the Coldfinger water exhauster is through the composition of the uncondensed vapor recirculating to the bottom section. Figure 6.2 shows the mass fraction of CH_4 in the recirculating stream as function of the top temperature for the minimum amount of stripping gas ($\beta = 0.001$) and an internal recirculation ratio of 0.8.
It can be seen that the mass fraction of CH_4 increases as the temperature in the top section decreases. This behavior means that at lower top temperatures, more water is condensed

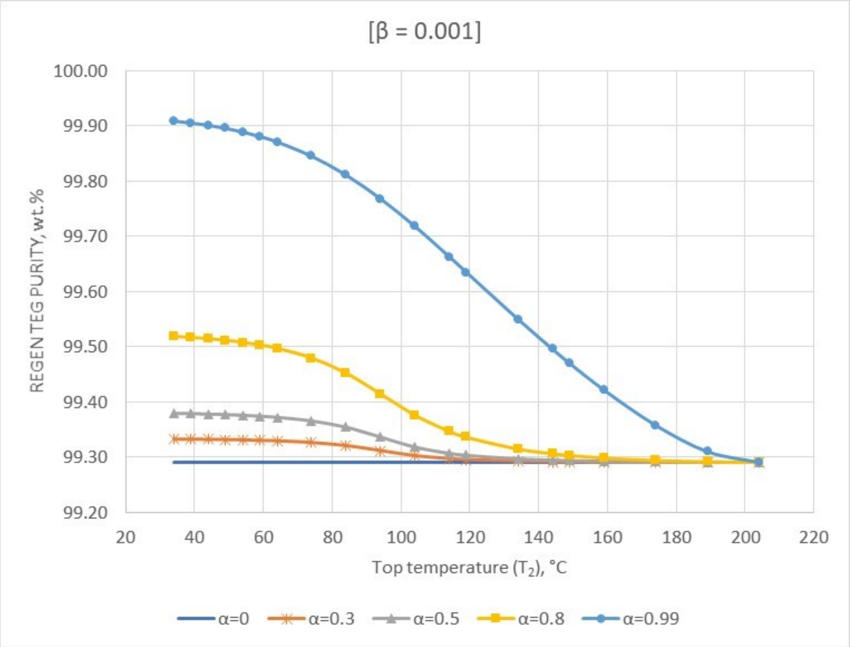

Figure 6.1: Influence of the temperature of the top section (T_2) on regenerated TEG purity obtained with the Coldfinger water exhauster, for different values of internal vapor recirculation (α) and β = 0.001

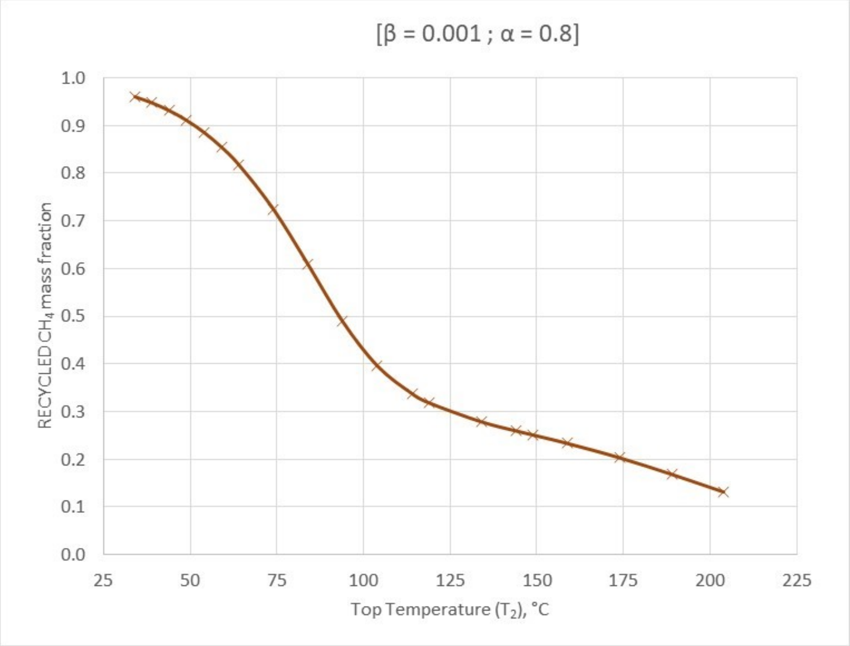

Figure 6.2: Influence of the temperature of the top section (T_2) on the composition of the recirculated vapor, for internal vapor recirculation ($\alpha = 0.8$) and β = 0.001

and removed from the vapor thus, the vapor recirculating to the bottom section is reacher in CH_4.

On the other hand, Figure 6.3 shows the effect of the top temperature on the composition of the recirculated vapor at the maximum internal recirculation ratio ($\alpha = 0.99$) and minimum amount of stripping gas injection ($\beta = 0.001$).
In this case, it is seen that the mass fraction of CH_4 in the uncondensed vapor decreases constantly as the temperature in the top section increases. This trend is maintained

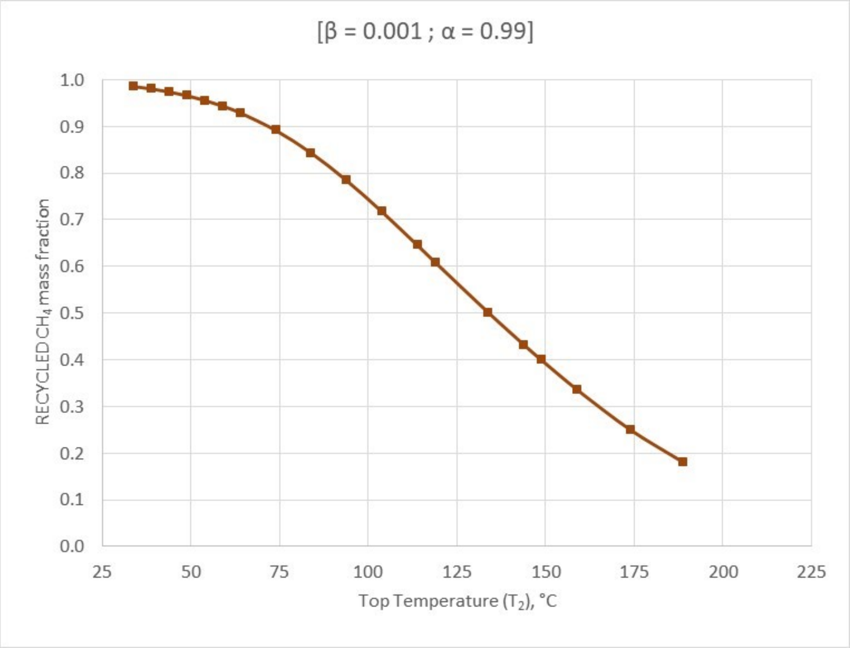

Figure 6.3: Influence of the temperature of the top section (T_2) on the composition of the recirculated vapor, for internal vapor recirculation ($\alpha = 0.99$) and β = 0.001

through all the temperature range under analysis, meaning that even at high temperatures of the top section, there is condensation of water. For instance, at top temperature of 150 °C, when $\alpha = 0.99$, the mass fraction of CH_4 is 0.4 while at the same top temperature, when $\alpha = 0.8$, the mass fraction of CH_4 is 0.2. This behavior explains the higher concentrations of TEG achieved considering an internal vapor recirculation ratio of 0.99, previously shown in Figure 6.1.

The effect of the top temperature can also be analyzed through the specific heat removed from the system. Figure 6.4 shows the purity of TEG as a function of the specific heat expressed per kilogram of liquid feed, for the case when the internal vapor recirculation ratio is 0.8 and the gas-to-feed liquid ratio is 0.001.
It is seen that this function presents an "S"-shaped curve, where the purity of TEG increases as more heat is removed from the system. In the first section of the curve, which corresponds to small amounts of heat removal and consequent high values of temperature at the top section, the purity of the regenerated TEG is almost constant meaning that water is not being condensed and sensible heat is removed from the system. As more heat is removed (top temperature decrease) the purity of TEG presents a sudden increase, meaning that at these values of top temperature, water is being condensed and latent heat is removed from the system. Finally, the value of TEG purity will reach a constant value, meaning that the removal of higher amounts of heat from the system will not have an effect in increasing the concentration of the regenerated TEG. This behavior is attributed to the exhaustion of water in the uncondensed vapor; in other words, an almost complete condensation of the water vapor in the proximity of the cooling pipe is achieved.

6.1.2 Effect of the stripping gas injection

According to data from current operating TEG dehydration plants with Coldfinger process, where rich TEG is most likely used as cooling media through the cold pipe, the

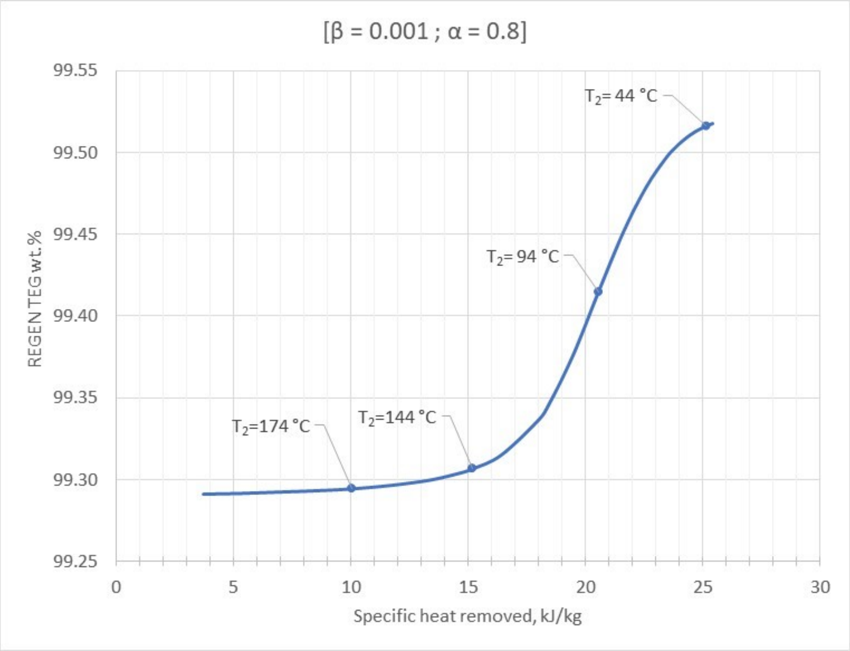

Figure 6.4: TEG purity as function of the specific heat removed from the system (per kilogram of liquid feed), for internal vapor recirculation ($\alpha = 0.8$) and β = 0.001

temperature increase of the cooling media is around 8 °C, which results in a temperature drop inside the equipment of approximately 145 °C ($T_2 = 59$°C). Moreover, if water is considered as an external cooling agent for the Coldfinger process, the maximum temperature drop achieved inside the equipment would be in the range of 170 °C ($T_2 = 34$°C). These values are taken into consideration for the further analysis of the operating parameters in the Coldfinger process. Figures 6.5 and 6.6 show the effect of the gas-to-feed liquid ratio in the performance of the Coldfinger water exhauster at the two values of top temperature before mentioned.

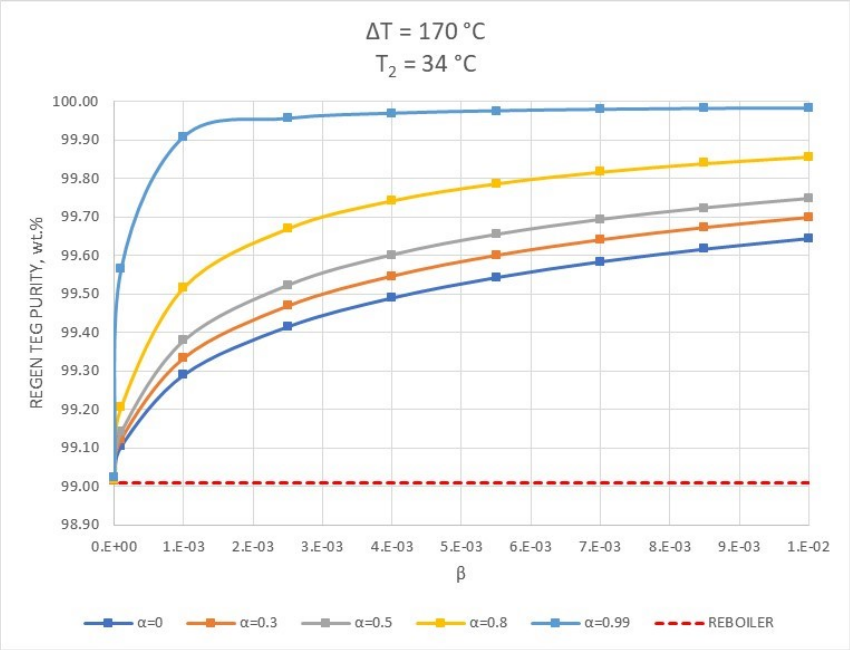

Figure 6.5: Variation of TEG purity (wt.%) as function of β, for different values of internal vapor recirculation, and top section temperature of 34°C

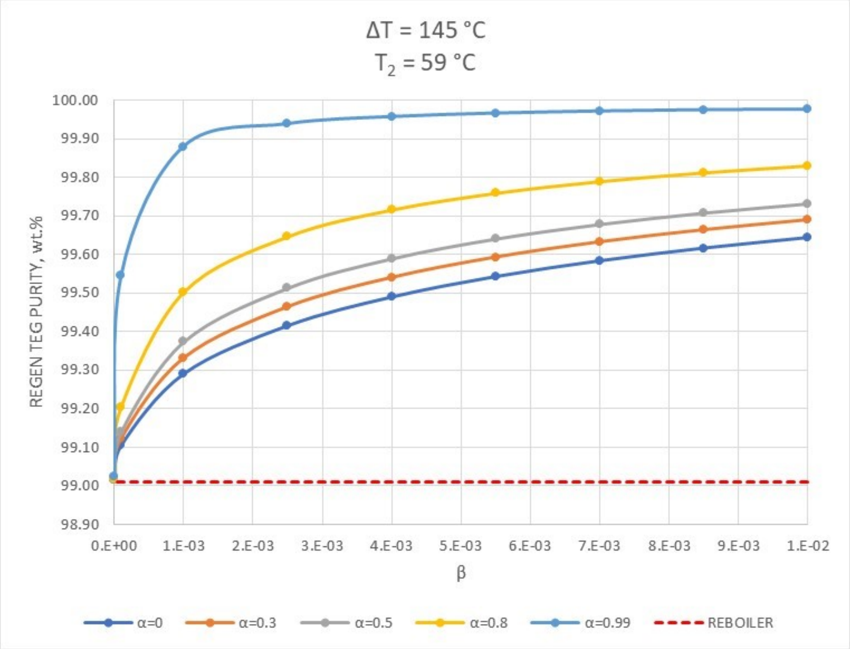

Figure 6.6: Variation of TEG purity (wt.%) as function of β, for different values of internal vapor recirculation, and top section temperature of 59°C

An additional value corresponding to a higher top temperature of 74 °C is also considered for analysis, and it is represented in Figure 6.7.

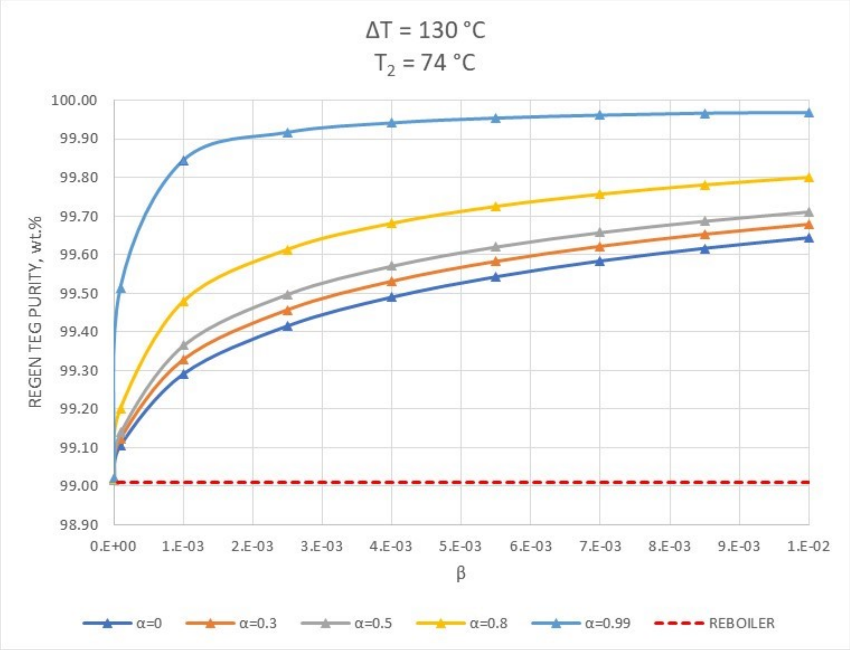

Figure 6.7: Variation of TEG purity (wt.%) as function of β, for different values of internal vapor recirculation, and top section temperature of 74°C

As it can be seen in Figures 6.5, 6.6 and 6.7, the purity of TEG increases as β and α increase as well. Furthermore, the mentioned figures present the purity of the liquid TEG leaving the reboiler of the regeneration column. It is clearly seen the significant enhancement in TEG purity achieved by means of the Coldfinger regeneration process and the influence of the top temperature in this behavior. It is seen that, even small amount of stripping gas injection generates a considerable reconcentration of TEG, having a bigger effect with lower temperatures in the top section. For instance, considering a value of β of 0.001 and a value of α of 0.99 (maximum internal vapor recirculatio ratio), the purity of TEG increases from 99.85 wt.% when T_2 is 74 °C to 99.91 wt.% when T_2 is 34 °C.

The maximum purity of TEG obtained by this means is 99.98 wt.%, corresponding to the case where the temperature at the top section is 34 °C (assumed maximum cooling), $\alpha = 0.99$ and $\beta = 0.01$, i.e. maximum amount of stripping gas injected.

From Figures 6.5, 6.6 and 6.7 it can also be seen that, for a given TEG purity, the amount of stripping gas necessary to inject into the Coldfinger is considerably less than the amount needed in a single-stage stripping process ($\alpha = 0$). For instance, for a TEG purity of 99.6 wt.% and T_2 of 34 °C, it would be necessary to inject into the Coldfinger a flow of dry gas equivalent to 0.2 % of the liquid feed (TEG entering the reboiler) considering an internal vapor recirculation of 0.8; while the same TEG purity (99.6 wt.%) would be achieved in a single-stage process by injecting a significant flow of dry gas equivalent to 0.8 % of the liquid feed.

These results demonstrate the validity of modeling the Coldfinger water exhauster as a two-stage phase equilibrium system, considering the internal vapor recirculation ratio and the injection of stripping gas.

6.2 HYSYS® Modeling Results

The conceptual modeling of the Coldfinger water exhauster was developed in the commercial process simulator Aspen HYSYS®. Since the EOS used for the HYSYS® modeling is not the same one used in the Matlab modeling, the analysis of the Coldfinger conceptual model was first performed considering a three-component system formed by $CH_4 - H_2O$-TEG.

Using the process flow diagram indicated in Figure 5.6, the variables α, β and top temperature (T_2) range were kept the same as the ones considered for the Matlab modeling study, in order to analyze the performance of the Coldfinger conceptualization within the commercial process simulator.
Similarly, the effect of the temperature of the top section was analyzed for different values of internal vapor recirculation ratio, as shown in Figure 6.8.
It can be seen that the behavior of the Coldfinger water exhauster in the commercial process simulator is similar to the one obtained in the conceptual modeling. There is, however, an unusual behavior for top section temperatures around 120 °C and 130 °C and $\alpha = 0.99$ which is not seen in the results obtained with Matlab. In general, the purity of the regenerated TEG decreases as the temperature of the top section increases, for all the values of α under study. For the case where $\alpha = 0$, the concentration of TEG is independent from the temperature T_2 since there is no vapor recirculating to the bottom section. Likewise, the highest TEG purity is achieved when the highest internal vapor recirculation ratio, $\alpha = 0.99$, is considered.

Also, the composition of the recirculated vapor as a function of top section temperature was analyzed. The results of the mass fraction of CH_4 in the recirculated vapor obtained with HYSYS set with the *Glycol fluid package* for the case where $\alpha = 0.8$ and $\alpha = 0.99$ are presented in Figures 6.9a and 6.9b, respectively.
It is also possible to see a decreasing concentration of CH_4 in the recirculating vapor as the temperature of the top section increases. Similarly to the results obtained with Matlab,

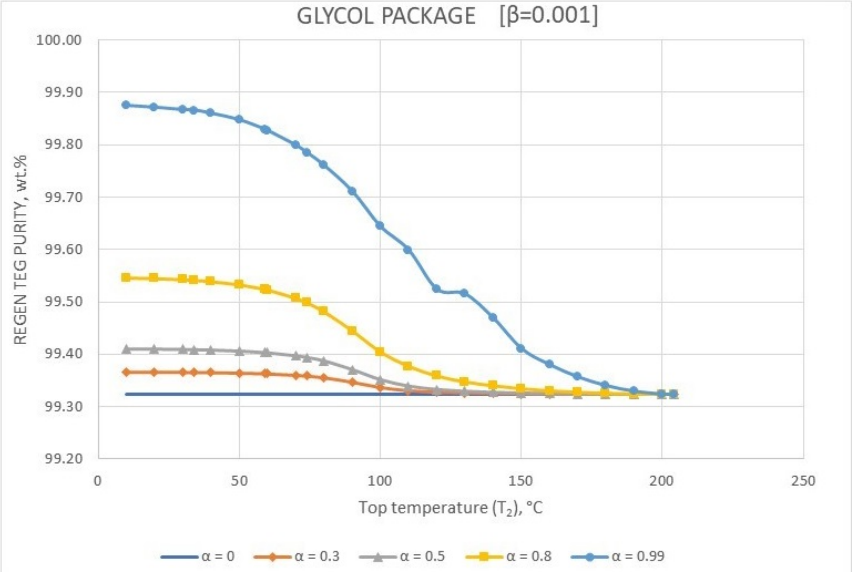

Figure 6.8: Variation of TEG purity (wt.%) as function of the top section temperature (T_2), for different values of internal vapor recirculation, and minimum gas-to-feed liquid ratio ($\beta = 0.001$) obtained with HYSYS®

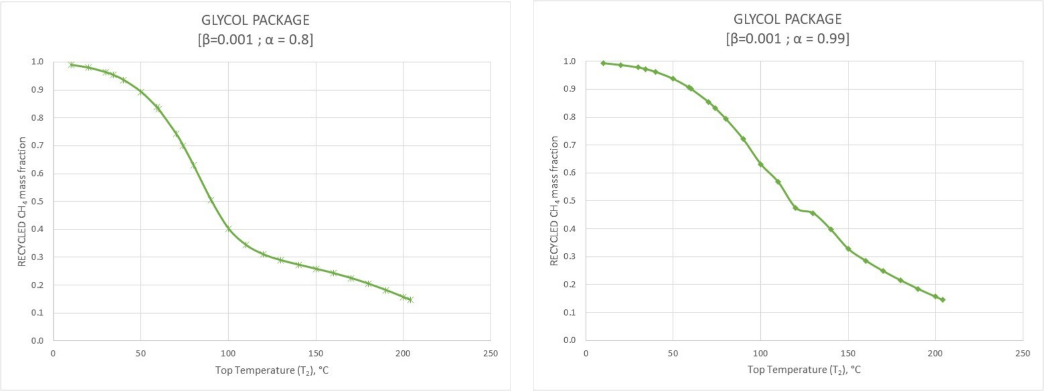

(a) $\alpha = 0.8$

(b) $\alpha = 0.99$

Figure 6.9: Concentration of CH_4 as function of the top section temperature (T_2) for $\beta = 0.001$, obtained with HYSYS®

the effect of T_2 in the composition of the uncondensed, recirculated vapor is stronger when the highest internal vapor recirculation ratio is considered ($\alpha = 0.99$). The unsual behavior for top section temperatures around 120 °C and 130 °C is also seen in this case.

The specific heat removal was analyzed as well for the HYSYS® simulation with the Glycol fluid package, considering $\alpha = 0.8$ and $\beta = 0.001$. As shown in Figure 6.10, the modeled Coldfinger water exhauster behaves in a similar way to the model in Matlab. The curve presented by the purity of TEG as a function of the top section temperature has also three main zones where a specific behavior can be distinguished. The first zone corresponds to high values of temperature in the top section where TEG concentration remains practically constant, due to the absence of water condensation. The second zone corresponds to decreasing values of top section temperature where TEG concentration increases abruptly as a consequence of the condensation of water in the vapor. Finally, the third zone corresponds to even lower values of temperature at the top section, where TEG purity achieves a maximum value since no more water is condensed and removed from the system.

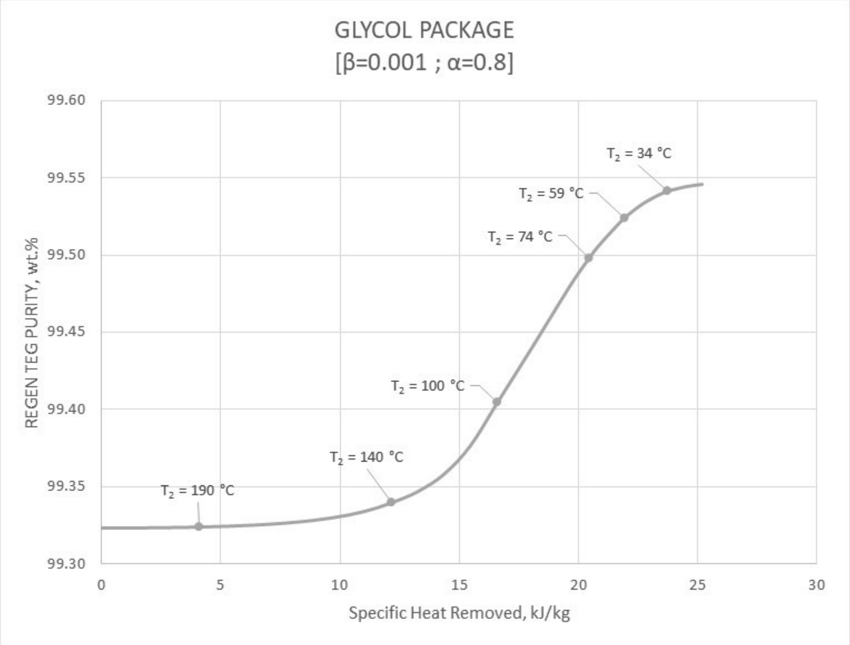

Figure 6.10: Purity of TEG (wt.%) as function of the specific heat removed from the system (per kilogram of liquid feed), for $\beta = 0.001$ and $\alpha = 0.8$ obtained with HYSYS®

Additionally, the effect of the injection of stripping gas in the behavior of the Coldfinger water exhauster was analyzed at the same three top temperatures (34, 59, 74 °C) considered in the Matlab study. The results are presented in Figures 6.11, 6.12 and 6.13.

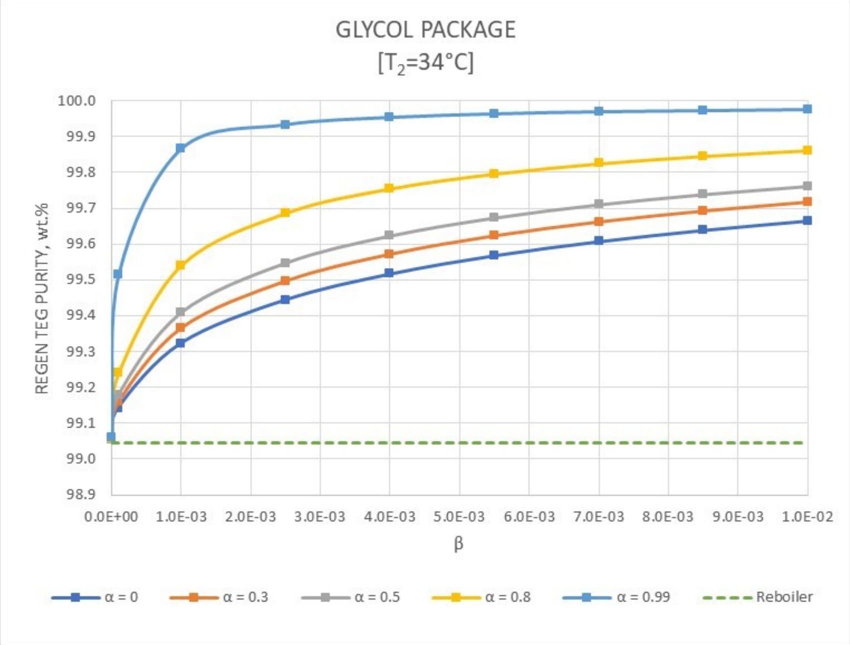

Figure 6.11: Purity of TEG (wt.%) as function of β, for different values of α and $T_2 = 34°C$ obtained with HYSYS®

It is clearly seen the similar behavior of the system obtained with the commercial process simulator. The purity of the regenerated TEG increases as β and α increase as well, reaching the maximum value of 99.97 wt.% purity when $\alpha = 0.99$, $\beta = 0.01$ and $T_2 = 34°C$. In these plots, it is also presented the concentration of TEG achieved under reboiler op-

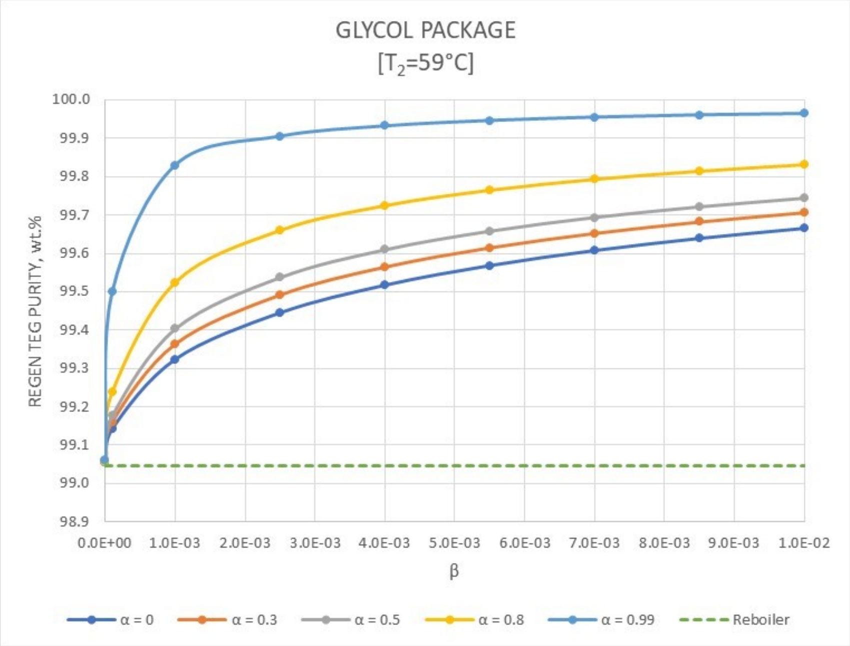

Figure 6.12: Purity of TEG (wt.%) as function of β, for different values of α and $T_2 = 59°C$ obtained with HYSYS®

Figure 6.13: Purity of TEG (wt.%) as function of β, for different values of α and $T_2 = 74°C$ obtained with HYSYS®

erating conditions, atmospheric pressure and 204 °C, with the Glycol fluid package, correspondent to 99.05 wt.%

6.3 Matlab-HYSYS® Comparative Analysis

The behavior of the Coldfinger water exhauster modeled using the process simulator HYSYS® with the Glycol fluid package, is similar to the one obtained for the same model using Matlab.

Even though a quantitative analysis between the results obtained with Matlab and the ones obtained with HYSYS® is not suitable due to the difference in the EOS implemented in each case, it is significant to perform a qualitative analysis of these results in order to observe the accuracy of the Coldfinger conceptualization.

The effect of the top temperature T_2 on the performance of the Coldfinger for both simulators, is shown in Figure 6.14.

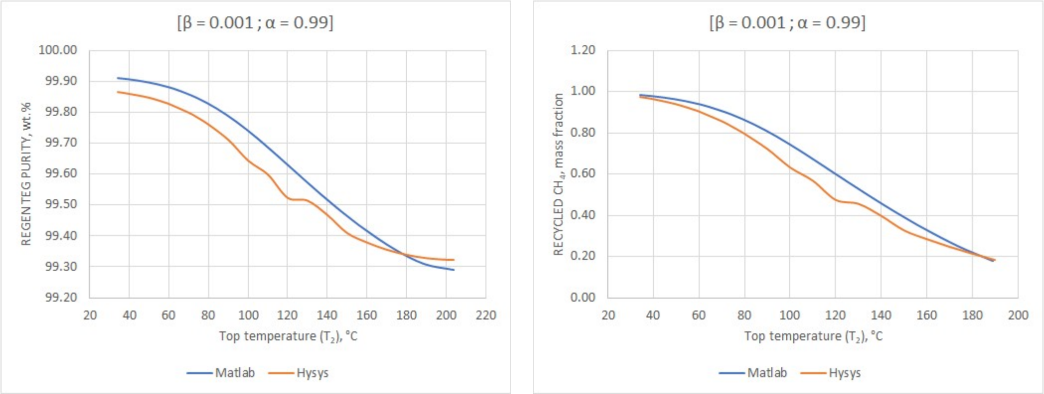

(a) Effect of T_2 on TEG purity; $\alpha = 0.99$, $\beta = 0.001$ **(b)** Effect of T_2 on CH4; $\alpha = 0.99$, $\beta = 0.001$

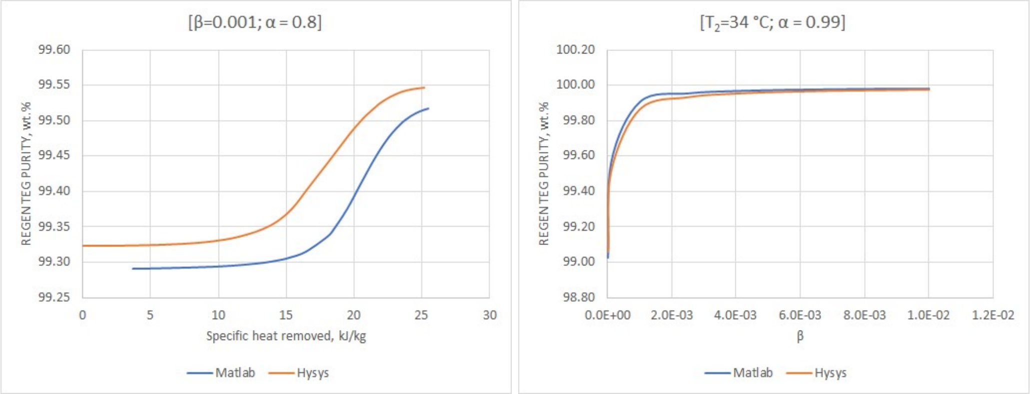

(c) Effect of specific heat removal; $\alpha = 0.8$, $\beta = 0.001$ **(d)** Effect of β on TEG purity; $\alpha = 0.99$

Figure 6.14: Results obtained with Matlab and HYSYS®

It is seen that the results obtained with Matlab and the ones with HYSYS® present a very similar trend in all the variables analyzed in this study. Consequently, it is possible to infer that the Coldfinger conceptualization can be accurately modeled as a two-stage phase equilibrium system through the Peng-Robinson equation of state with PT-Flash calculations in Matlab.

6.4 Modeling of the Gas dehydration process with HYSYS®

The gas dehydration process with the conceptual model of the Coldfinger water exhauster for the regeneration of TEG, is simulated in HYSYS®. The process flow diagram built is presented in Figure 6.15.

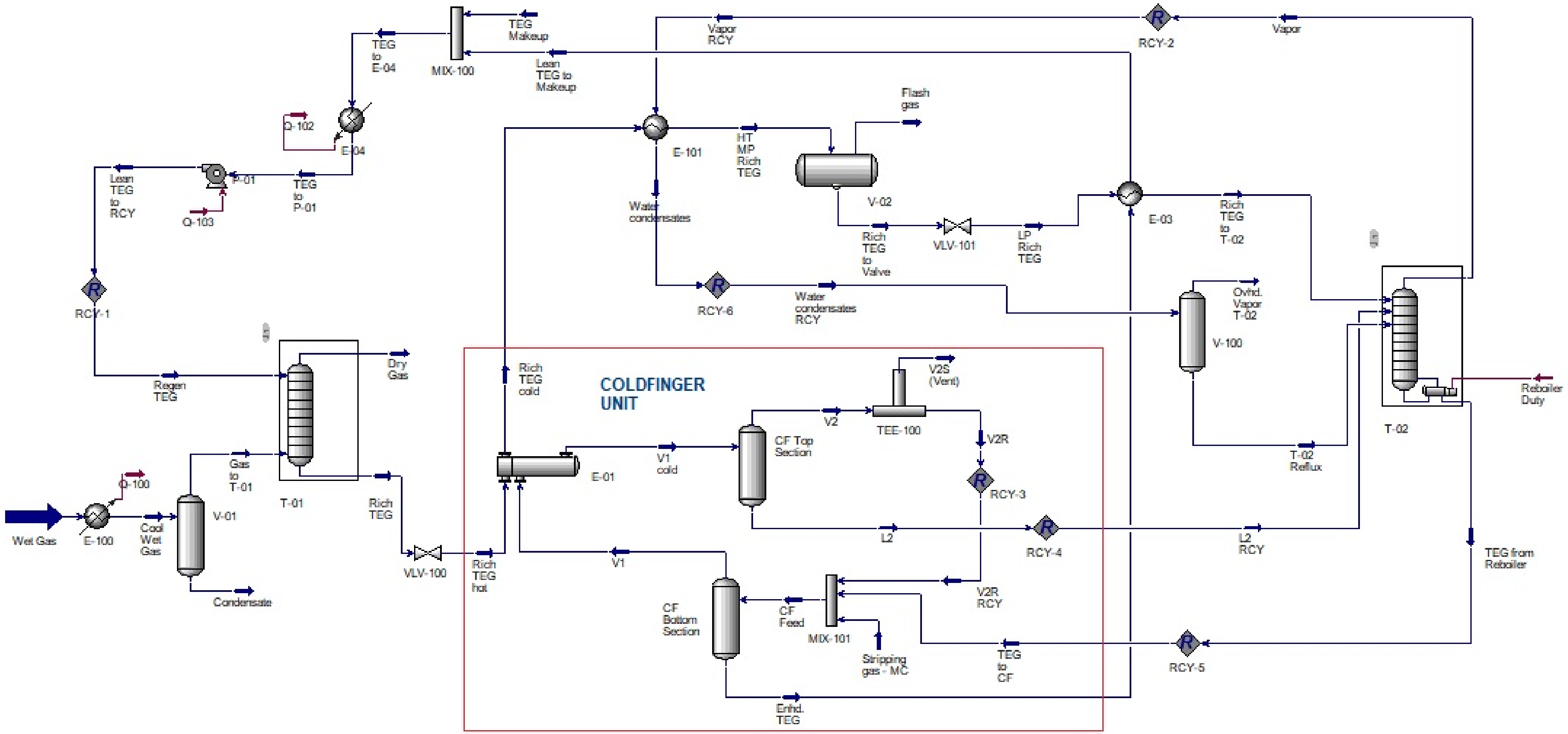

Figure 6.15: Process flow diagram of the gas dehydration process with Coldfinger water exhauster, for simulation in HYSYS®

As mentioned in section 5.5 of this report, eight simulation cases are considered for analysis of the Coldfinger conceptual modeling in a gas dehydration unit. The results obtained for all the cases are summarized in Table 6.1.

Table 6.1: Performance of the Coldfinger water exhauster in a natural gas dehydration process - HYSYS®

Case	Stripping gas flow, kg/h	Regen.TEG purity, wt.%	Strip. gas composition	α	β
Base case 1	6.01	99.30	CH_4	0	0.001
Base case 2	6.01	99.25	Dry gas	0	0.001
Case 3	6.56	99.82	CH_4	0.99	0.001
Case 4	6.50	99.76	Dry gas	0.99	0.001
Case 5	6.38	99.51	CH_4	0.8	0.001
Case 6	6.37	99.43	Dry gas	0.8	0.001
Case 7	280.64	99.82	CH_4	0	0.045
Case 8	298.62	99.76	Dry gas	0	0.049

As it can be seen in Table 6.1, for a fixed value of α and β (cases 1 to 6), the regeneration of TEG is influenced by the composition of the stripping gas injected into the bottom section of the Coldfinger. For instance, TEG purity achieved in Case 3 ($\alpha = 0.99$, $\beta = 0.001$) where the stripping gas is pure CH_4 is higher than the TEG purity achieved in Case 4 ($\alpha = 0.99$, $\beta = 0.001$) where the stripping gas is a multicomponent stream consisting of methane, ethane, propane and other hydrocarbons up to C6. Similar behavior is observed in Cases 5 and 6 with $\alpha = 0.8$, $\beta = 0.001$, stripping gas pure CH_4 and multicomponent gas stream, respectively. In addition, it is seen that the purity of TEG using Coldfinger water exhauster is significantly increased with respect to the TEG reconcentration achieved with a single-stage gas stripping process (Base case 1 and 2), confirming the advantage of the Coldfinger for enhanced regeneration of TEG over the conventional process.

Additionally, the requirement of stripping gas is analyzed for two additional cases (Case 7 and Case 8) that represent single-stage stripping processes. The base of comparison considered is the purity of TEG achieved in Case 3 and Case 4, corresponding to the cases where maximum TEG purity is achieved using pure CH_4 and multicomponent gas stream as stripping gas, respectively. As it can be seen in Table 6.1, when methane is injected as stripping gas, as in Cases 3 and 7, the amount of gas necessary in the conventional stripping process to achieve the same TEG purity achieved with the Coldfinger water exhauster ($\alpha = 0.99$, $\beta = 0.001$) is approximately 43 times higher. Moreover, when a multicomponent gas stream is injected for stripping, as in Cases 4 and 8, the amount of gas necessary in the conventional stripping process to achieve the same TEG purity achieved with the Coldfinger water exhauster ($\alpha = 0.99$, $\beta = 0.001$) is approximately 45 times higher.

In brief, these results demonstrate that the modeling of the Coldfinger water exhauster is influenced by the internal vapor recirculation ratio, amount and nature of the stripping gas injected to the bottom of the water exhauster, and the temperature of the top section of the vessel.

7 Conclusions

Modeling the Coldfinger water exhauster as a two-stage phase equilibrium system in Matlab and HYSYS® presents the expected behavior for regeneration of TEG, increasing its concentration with respect to the one obtained at reboiler conditions of pressure and temperature. Considering a simplified ternary system of CH_4-H_2O-TEG, the natural convection inside the vessel and the injection of stripping gas, it is shown how the Coldfinger water exhauster is able of increasing the purity of TEG in the regeneration process by using only small quantities of dry gas.

The maximum TEG purity achieved using Matlab is 99.98 wt.%, considering an internal vapor recirculation ratio of 0.99, a temperature of the top section of 34 °C and a gas-to-feed liquid ratio of 0.01. These correspond to the maximum values of vapor recirculation ratio, cooling and amount of stripping gas injected, respectively.

The maximum TEG purity achieved using HYSYS® is 99.97 wt.%, considering an internal vapor recirculation ratio of 0.99, a temperature of the top section of 34 °C and a gas-to-feed liquid ratio of 0.01. Similarly, these correspond to the maximum values of vapor recirculation ratio, cooling and amount of stripping gas injected, respectively.

The qualitative comparison between the results obtained with Matlab and HYSYS® demonstrates that the Coldfinger can be accurately modeled as a two-stage phase equilibrium system through the Peng-Robinson equation of state with PT-Flash calculations in Matlab.

Through the in-depth study of the parameters influencing the performance of the Coldfinger, it is seen that the internal vapor recirculation, along with the constant condensation of water on the surface of the cooling coil, exerts a strong influence on the achievable levels of TEG dehydration. These parameters are, in fact, the key conceptual parameters to explain the extent of the enhanced TEG regeneration with small amounts of injected dry gas. The heat removed from the top section of the vessel shows, as well, that the purity of TEG depends strongly on the condensation capacity of the cooling pipe.

The expected behavior of the Coldfinger conceptualization is also observed when it is implemented in the TEG regeneration process of a gas dehydration unit, considering a multicomponent gas. It is seen the effect of the composition of the stripping gas in the performance of the Coldfinger. Higher concentrations of TEG are achieved when pure CH_4 is injected as stripping gas.

The results presented in this work demonstrate that it is possible to explain the behavior of the Coldfinger water exhauster based on thermodynamics. Therefore, a conceptual modeling of the Coldfinger water exhauster is successfully achieved by representing the equipment as a two-stage phase equilibrium system with internal recirculation of the vapor and different stage temperatures.

Bibliography

[1] GPSA, *Engineering Data Book*. Gas Processors Suppliers Association, 2004. ISBN: 978-1-85617-980-5.

[2] F. Manning and R. Thomson, *Oilfield Processing of Petroleum. Volume One: Natural Gas*. Pennwell Publishing Company, 1991. ISBN: 0-87814-342-2.

[3] F. Gironi, M. Maschietti, V. Piemonte, D. Diba, S. Gallegati, and S. Schiavo, *Triethylene glycol regeneration in natural gas dehydration plants: a study on the Coldfinger process*. Proceedings of the 8th Offshore Mediterranean Conference and Exhibition, 2007. Ravenna, Italy.

[4] I. Gil, J. Guevara, J. Garcia, A. Leguizamon, and G. Rodriguez, *Process Analysis and Simulation in Chemical Engineering*. Springer, 2016. ISBN: 978-3-319-14811-3.

[5] M. Stewart and K. Arnold, *Gas Dehydration Field Manual*. Gulf Professional Publishing, 2011. ISBN: 978-1-85617-980-5.

[6] K. Arnold and M. Stewart, *Surface Production Operations. Volume 2: Design of Gas-Handling Systems and Facilities*. Elsevier Science / Originally published by Gulf Publishing Company, 1999. ISBN:0-88415-822-5.

[7] J. Campbell, *Gas Conditioning and Processing. Volume 2: The Equipment Modules*. Campbell Petroleum Series, 1992.

[8] A. Rojey, C. Jaffret, S. Cornot-Gandolphe, B. Durand, S. Jullina, and M. Valais, *Natural Gas: Production, Processing, Transport*. Editions Technip, 1997. ISBN: 2-7108-0693-2.

[9] B. Guo and A. Ghalambor, *Natural Gas Engineering Handbook, Second edition*. Gulf Publishing Company, 2012. ISBN: 978-1-933-762-21-8.

[10] L. Reid, *Method for removing water from glycol solutions*. US Patent 4332643, 1982.

[11] J. Smith, H. V. Ness, and M. Abbott, *Introduction to Chemical Engineering Thermodynamics*. McGraw-Hill Higher Education, 2001. ISBN: 0-07-240296-2.

[12] H. Orbey and S. Sandler, *Modeling Vapor-Liquid Equilibria: Cubic Equations of State and Their Mixing Rules*. Cambridge Series in Chemical Engineering, 1998. ISBN: 0-521-62027-9.

[13] AspenTechnology, *HYSYS® 2004.2 User Manual - Simulation Basis*. Aspen Technology, 2005.

[14] J.-N. Jaubert, S. Vitu, F. Mutelet, and J.-P. Corriou, *Extension of the PPR78 model (predictive 1978, Peng–Robinson EOS with temperature dependent kij calculated through a group contribution method) to systems containing aromatic compounds*. Fluid Phase Equilibria, 2005. 237, 193-211.

[15] L. Reid, *Apparatus for dehydrating organic liquids*. US Patent 3589984, 1971.

[16] L. Øi and E. Selstø, *Process simulation of glycol regeneration*. for presentation at GPA Europe's meeting, 2002.

[17] M. Rahimpour, S. Jokar, P. Feyzi, and R. Asghari, *Investigating the performance of dehydration unit with Coldfinger technology in gas processing plant*. Journal of Natural Gas Science and Engineering, 2013. 12, 1-12.

[18] R. Perry and D. G. (Eds.), *Perry's Chemical Engineers' Handbook*. McGraw-Hill, 1997. ISBN: 0-07-115448-5.

[19] F. Gironi, M. Maschietti, and V. Piemonte, *Natural gas dehydration: a triethylene glycol-water system analysis*. Energy Sources, Part A: Recovery, Utilization, and Environmental Effects, 2010. 32:20, 1861 - 1868.

[20] F. Gironi, M. Maschietti, and V. Piemonte, *Modelling of triethylene glycol – water system for natural gas dehydration*. Chemical Engineering Transactions, 2007. 11, 881-886.

[21] F. Jou, R. Deshmukh, F. Otto, and A. Mather, *Vapor-liquid equilibria for acid gases and lower alkanes in triethylene glycol*. Fluid Phase Equilibria, 1987. 36, 121-140.

[22] O. Culberson and J. McKetta, *Phase equilibria in hydrocarbon-water systems III – The solubility of methane in water at pressures to 10,000 psia*. Petroleum Transactions,AIME, 1951. 192, 223-226.

[23] C. Yaws, *Chemical Properties Handbook: Physical, Thermodynamic, Environmental, Transport, Safety, and Health Related Properties for Organic and Inorganic Chemicals*. McGraw-Hill, 1999. ISBN: 0-07-073401-1.